AD_____

AWARD NUMBER: **W81XWH-12-1-0282**

TITLE: **Monoamine Oxidase A: A Novel Target for Progression and Metastasis of Prostate Cancer**

PRINCIPAL INVESTIGATOR: **Jean C. Shih, Ph.D.**

CONTRATING ORGANIZATION: **University of Southern California**
Los Angeles, CA 90089-0001

REPORT DATE: **October 2013**

TYPE OF REPORT: **Annual**

PREPARED FOR: **U.S. Army Medical Research and Materiel Command**
Fort Detrick, Maryland 21702-5012

REPORT DOCUMENTATION PAGE

Form Approved
OMB No. 0704-0188

1. REPORT DATE	2. REPORT TYPE	3. DATES COVERED
October 2013	Annual	30September2012–29September2013

4. TITLE AND SUBTITLE
Monoamine Oxidase A: A Novel Target for Progression and Metastasis of Prostate Cancer

5a. CONTRACT NUMBER
W81XWH-12-1-0282

5b. GRANT NUMBER
W81XWH-12-1-0282

5c. PROGRAM ELEMENT NUMBER

6. AUTHOR(S)
Dr. Jean C. Shih
Dr. Bogdan Z. Olenyuk

E-Mail: jcshih@usc.edu and bogdan@usc.edu

5d. PROJECT NUMBER

5e. TASK NUMBER

5f. WORK UNIT NUMBER

7. PERFORMING ORGANIZATION NAME(S) AND ADDRESS(ES)

University of Southern California
3720 S. Flower Street
Los Angeles, CA 90089-0001

8. PERFORMING ORGANIZATION REPORT NUMBER

9. SPONSORING / MONITORING AGENCY NAME(S) AND ADDRESS(ES)
U.S. Army Medical Research and Materiel Command
Fort Detrick, Maryland 21702-5012

10. SPONSOR/MONITOR'S ACRONYM(S)

11. SPONSOR/MONITOR'S REPORT NUMBER(S)

12. DISTRIBUTION / AVAILABILITY STATEMENT
Approved for Public Release; Distribution Unlimited

13. SUPPLEMENTARY NOTES

14. ABSTRACT

The purpose of this project is investigation of the critical role of the enzyme monoamine oxidase A (MAOA) in the progression and metastasis of prostate cancer. Throughout the Year 1 of this study we focused on study of the functional and mechanistic roles of MAOA in epithelial-to-mesenchymal transition (EMT), elevated production of reactive oxygen species (ROS), and its effect on hypoxia-inducible factor 1α (HIF1α). We established and characterized stable wild-type and MAOA-knockdown human prostate cancer cells. Using our established cell lines we analyzed wild-type and MAOA-knockdown humaen prostate cancer xenograft specimens. We also designed, developed and tested in vitro a novel pharmacological inhibitor of MAOA though chemical synthesis of the conjugate of MAO inhibitor clorgyline and near-infrared dye MHI-148. We found that inhibition of MAOA activity with this novel compound results in robust suppression of the prostate cancer cell growth and colony formation.

15. SUBJECT TERMS none provided

16. SECURITY CLASSIFICATION OF:			17. LIMITATION OF ABSTRACT	18. NUMBER OF PAGES	19a. NAME OF RESPONSIBLE PERSON
a. REPORT	b. ABSTRACT	c. THIS PAGE			19b. TELEPHONE NUMBER *(include area code)*
U	U	U	UU	67	USAMRMC

Table of Contents

1. **INTRODUCTION: Monoamine Oxidase A (MAOA)**, the subject of the present study, is a mitochondria-bound enzyme that oxidatively deaminates monoamine neurotransmitters and dietary amines and produces hydrogen peroxide, a major source of reactive oxygen species (ROS).(*1, 2*) ROS causes DNA damage and tumor initiation.(*3-5*) **The purpose of this research** is twofold: 1) to seek fundamental mechanistic insights on the functional roles of MAOA in human PCa progression and metastasis, and 2) to design and develop novel and effective tumor-specific pharmacological inhibitor of MAOA and to determine its effect on PCa tumor growth and metastasis in tumor xenograft mouse models. **The scope of this research** involves experiments and assays to study the role of MAOA in PCa progression and metastasis in vitro [LNCaP (androgen-sensitive) and C4-2B (derived from LNCaP, androgen-insensitive) and PC3 (androgen-insensitive) PCa cells] and in vivo [tumor growth studies, and tumor metastasis to bone and soft tissues] studied in mice. (*6, 7*)

2. **KEYWORDS:** Prostate cancer (PCa), Monoamine Oxidase A (MAOA), MHI-clorgyline, near-infrared (NIR) emitting compound, novel target, novel therapeutic agent, HIF-1α., reactive oxygen species (ROS), hydrogen peroxide (H_2O_2).

3. **OVERALL PROJECT SUMMARY:**

The objective of this study is investigation of the functional and mechanistic roles of MAOA in human PCa growth and metastasis, with the focus on epithelial-to-mesenchymal transition (EMT), reactive oxygen species (ROS), hypoxia-inducible factor 1α (HIF1α) and biomarkers associated with PCa progression. Furthermore, we designed, synthesized and tested *in vitro* and *in vivo* a novel tumor-specific MAOA inhibitor-near infrared (NIR) dye inhibitor (NIR-MAOA inhibitor), called MHI-clorgyline, with the goal to target and image advanced and metastatic PCa in our animal models. The reported study was conducted by three collaborating labs from two organizations (the Shih lab at USC, the Zhau lab at CSMC, and the Olenyuk lab at USC). **The Shih lab** was responsible for determining MAOA effects on PCa tumor growth and metastasis in tumor xenograft mouse models and assessing the efficacy of NIR-MAOA inhibitor on tumor growth and metastasis in tumor xenograft mouse models. **The Zhau lab** was responsible for generating different genetically manipulated human PCa cell lines and assisting with extensive immunohistochemical (IHC) analysis of tumor specimens with PCa-associated biomarkers for tumor xenograft studies. **The Olenyuk lab** was responsible for chemically synthesizing and characterizing NIR-MAOA inhibitor and assisting with determination of their pharmacological effects on PCa in tumor xenograft studies.

The progress during the Year 1 of this project in accordance with the detailed task assignments, as presented in SOW, is described below:

Task 1. (**Specific Aim 1A**): Determination of the effects of MAOA on human prostate tumor growth and metastasis.

1a. Establishment, validation and characterization of stable wild-type (WT) and MAOA-knockdown (KD) PCa cells (LNCaP, C4-2 and $ARCaP_M$) genetically engineered with luciferase (luc) for tumor — Months 1-6

xenograft studies. Investigator: Haiyen Zhau (CSMC)

1b. Prostate tumor growth studies: **orthotopic injection** of WT and MAOA-KD PCa cells into the athymic nude mice, determination of tumor growth post-injection by serial imaging of luciferase bioluminescence, determination of tumor ROS levels at sacrifice, and IHC analysis of tumor specimens post-sacrifice (cell proliferation, EMT and hypoxia markers). Investigators: Haiyen Zhau (CSMC) and Jean Shih (USC) — Months 7-12

1c. Prostate tumor metastasis studies: **intracardiac injection** of PCa cells into athymic nude mice, determination of tumor bone metastasis status and tumor osteolesion post-injection by serial imaging of luc bioluminescence and X-ray, and IHC analysis of tumor/bone specimens post-sacrifice (osteoclastic, osteoblastic, EMT and hypoxia markers). Investigators: Haiyen Zhau (CSMC) and Jean Shih (USC) — Months 7-12

Task 3 (**Specific Aim 2**): Synthesis and characterization of novel near-infrared (NIR) dye-clorgyline conjugate, and determination of its *in vivo* inhibitory effects on tumor growth and metastasis in tumor xenograft mouse models.

3a. Design, synthesis and chemical characterization of NIR-clorgyline.
Investigator: Bogdan Olenyuk (USC) — Months 1-6

3b. Determination of MAOA inhibition curves in human PCa cells. Investigator: Jean Shih (USC) — Months 7-12

3c. Determination of the cellular uptake and localization of MAOA inhibitor – NIR dye conjugate (NIR-clorgyline) in human PCa cells. Investigator: Bogdan Olenyuk (USC) — Months 9-12

Task 1a: We established and characterized stable wild-type and MAOA-knockdown human prostate cancer cells (C4-2 and $ARCaP_M$) for animal studies. We utilized lentiviral particles that express pGL4 Luciferase Reporter Vectors (Promega) to infect both C4-2 and $ARCaP_M$ cells followed by selection for stable clones with hygromycin. Successful stable engineering of luciferase gene into the genome of these cells was validated by luciferase assay. These luc-labeled cells, when injected into mice, will be visualized by bioluminescence imaging. Next, these cells were infected with lentiviral particles that express specific shRNAs targeting MAOA (Sigma-Aldrich) followed by selection for stable clones with puromycin, and wild-type control cells were infected with control lentiviral particles (Sigma-Aldrich) accordingly. Successful knockdown of MAOA in these cells were examined by Western blot by probing MAOA protein. Furthermore, cell proliferation, invasion and migration were determined in these wild-type and MAOA-knockdown cells, and knockdown of MAOA significantly reduced these indices in both C4-2 and $ARCaP_M$ cells (Figure 1). These cells are now ready to be used in proposed animal studies, such as intratibial injection for investigating MAOA-mediated prostate cancer-bone cell interaction.

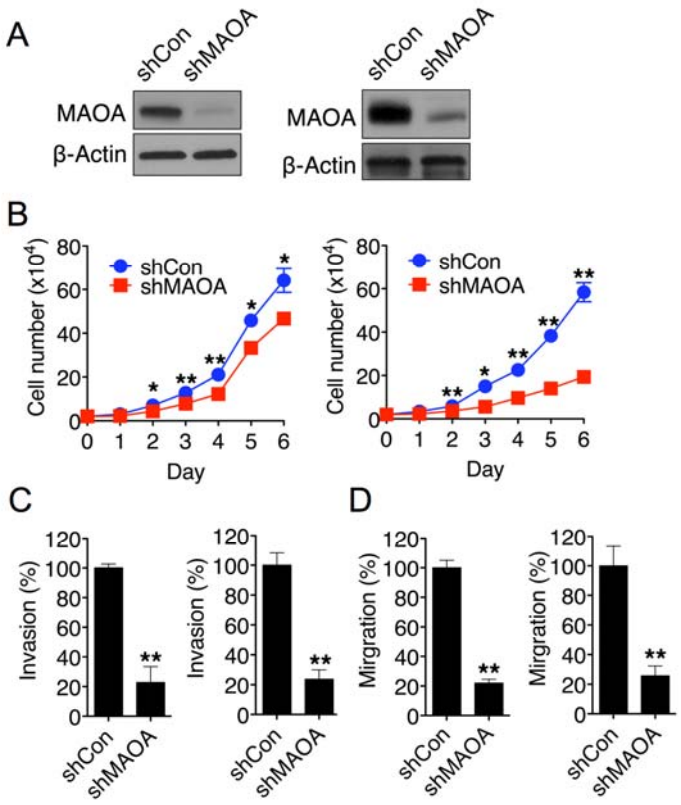

Figure 1. Wild-type (shCon) and MAOA-knockdown (shMAOA) C4-2 (left panel) and $ARCaP_M$ (right panel) cells were characterized with MAOA protein expression (A), cell proliferation (B), cell invasion (C) and cell migration (D).

Task 1b: ***We analyzed wild-type and MAOA-knockdown human prostate cancer xenograft specimens with focuses on cell proliferation, epithelial-mesenchymal transition (EMT) and hypoxia signaling.*** Our preliminary *in vitro* results showed that MAOA is engaged in EMT induction and HIF1α stabilization in human prostate cancer cells, we therefore analyzed wild-type and MAOA-knockdown human prostate LNCaP and C4-2 subcutaneous tumor xenograft specimens with select EMT and hypoxia markers by immunohistochemical (IHC) analyses. Our results showed that knockdown of MAOA significantly decreased the expression levels of Ki-67 (a cell proliferation marker), Vimentin (a mesenchymal marker), HIF1α and VEGF-A (a HIF1α target gene), but increased E-cadherin (an epithelial marker) (Figure 2), which are consistent to the *in vitro* findings and confirm MAO A effect in driving EMT and hypoxia.(*8*)

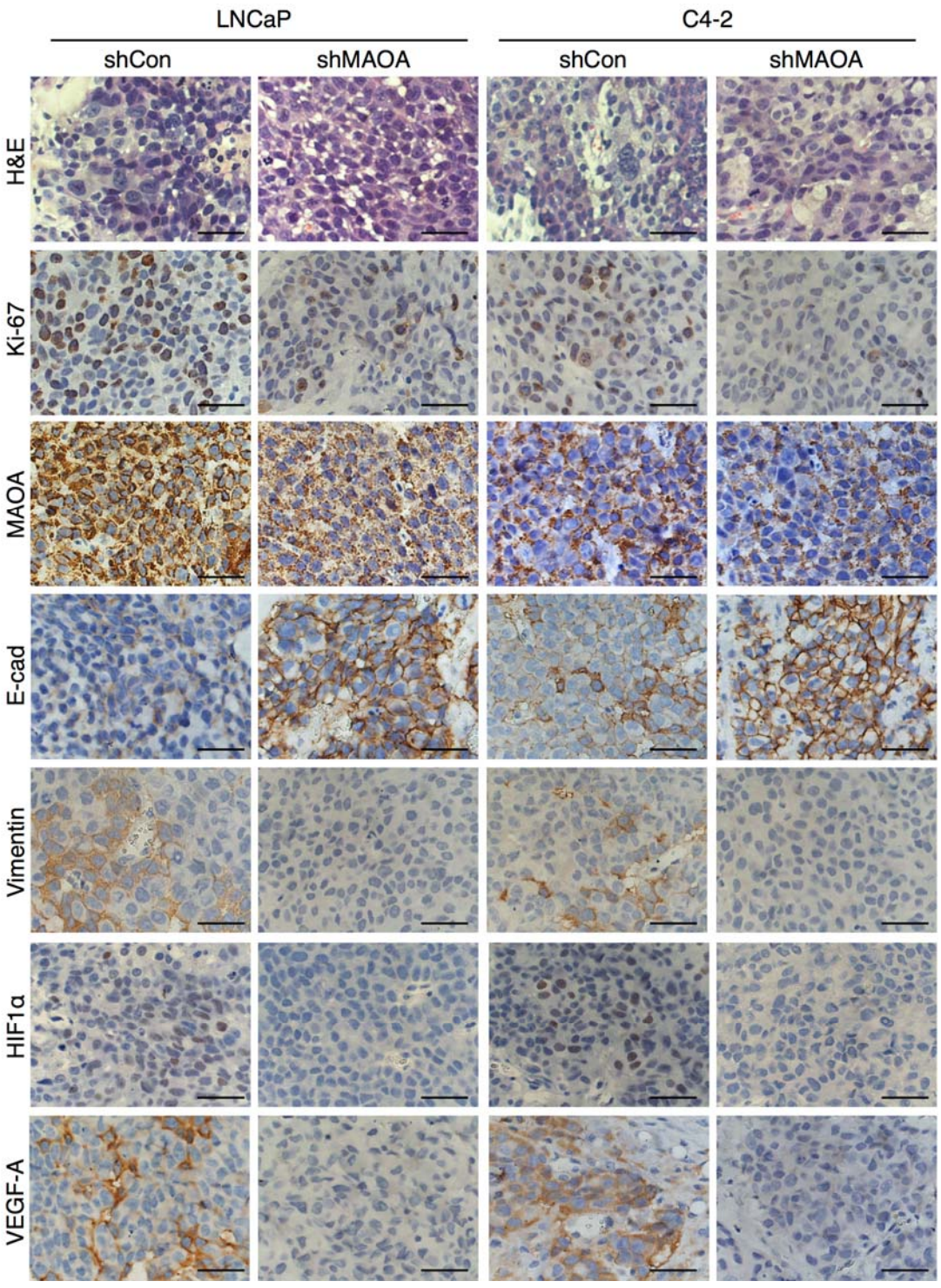

Figure 2. H&E and IHC analyses of Ki-67, MAOA, E-cadherin, Vimentin, HIF1α and VEGF-A expression in wild-type (shCon) and MAOA-knockdown (shMAOA) LNCaP (left panel) and C4-2 (right panel) tumor xenografts. Representative images from five separate samples are shown. Original magnification, x500; scale bar: 20 μm.

Task 1c: We studied prostate tumor metastasis though **intracardiac injection** of PCa cells into the athymic nude mice. Briefly, mice were injected intracardially with MAO A knockdown $ARCaP_M$ cells (*9*) and control wild-type cells. Our preliminary studies show that knockdown of MAO A in $ARCaP_M$ cells reduced the rate of prostate cancer cell metastasis (Figure 3). This experiment is still ongoing.

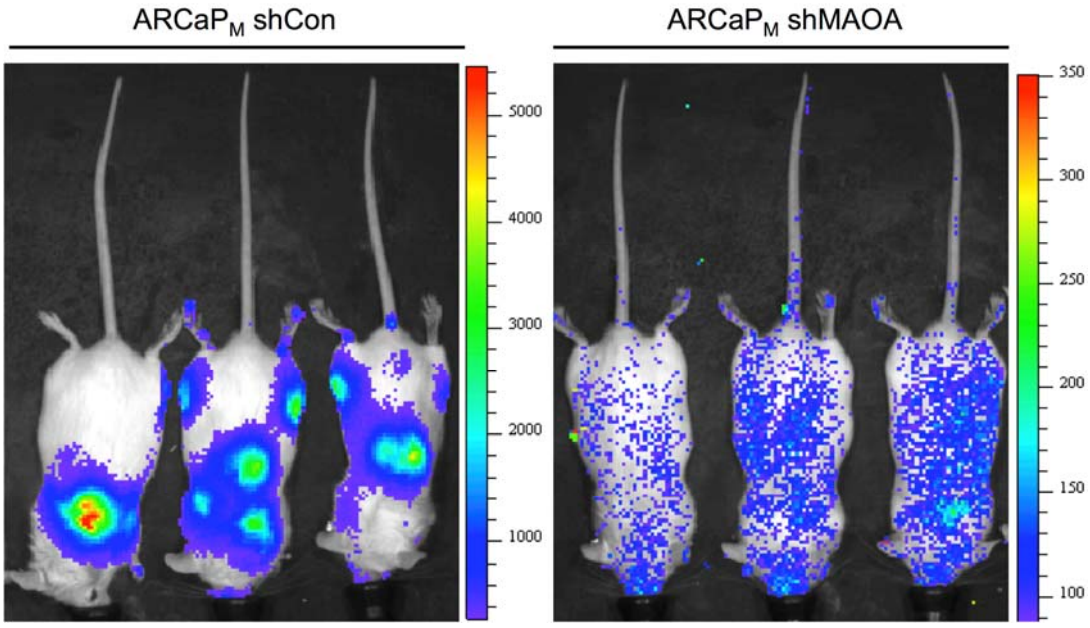

Figure 3. MAOA knockdown reduces the metastasis rate of PCa cells injected intracardially. Left: images of mice injected with control $ARCaP_M$ cells (shCon) and showing significant degree of metastasis. Right: images of mice injected with $ARCaP_M$ MAO KD cells.

Task 3 (**Specific Aim 2**): This Specific Aim was focused on design and synthesis of novel clorgyline (a potent MAOA inhibitor) - near-infrared (NIR) dye conjugate (NIR-clorgyline) specifically targeting tumors. We also determined the inhibitory effect of this conjugate on tumor growth and metastasis of human PCa in tumor xenograft mouse models.

Task3a: Based on crystal structure of MAOA (*10*) we designed a novel clorgyline-NIR dye conjugate and prepared it through a series of synthetic steps as shown in Scheme 1. A modified clorgyline functionality was prepared first in order to accomplish this conjugation:

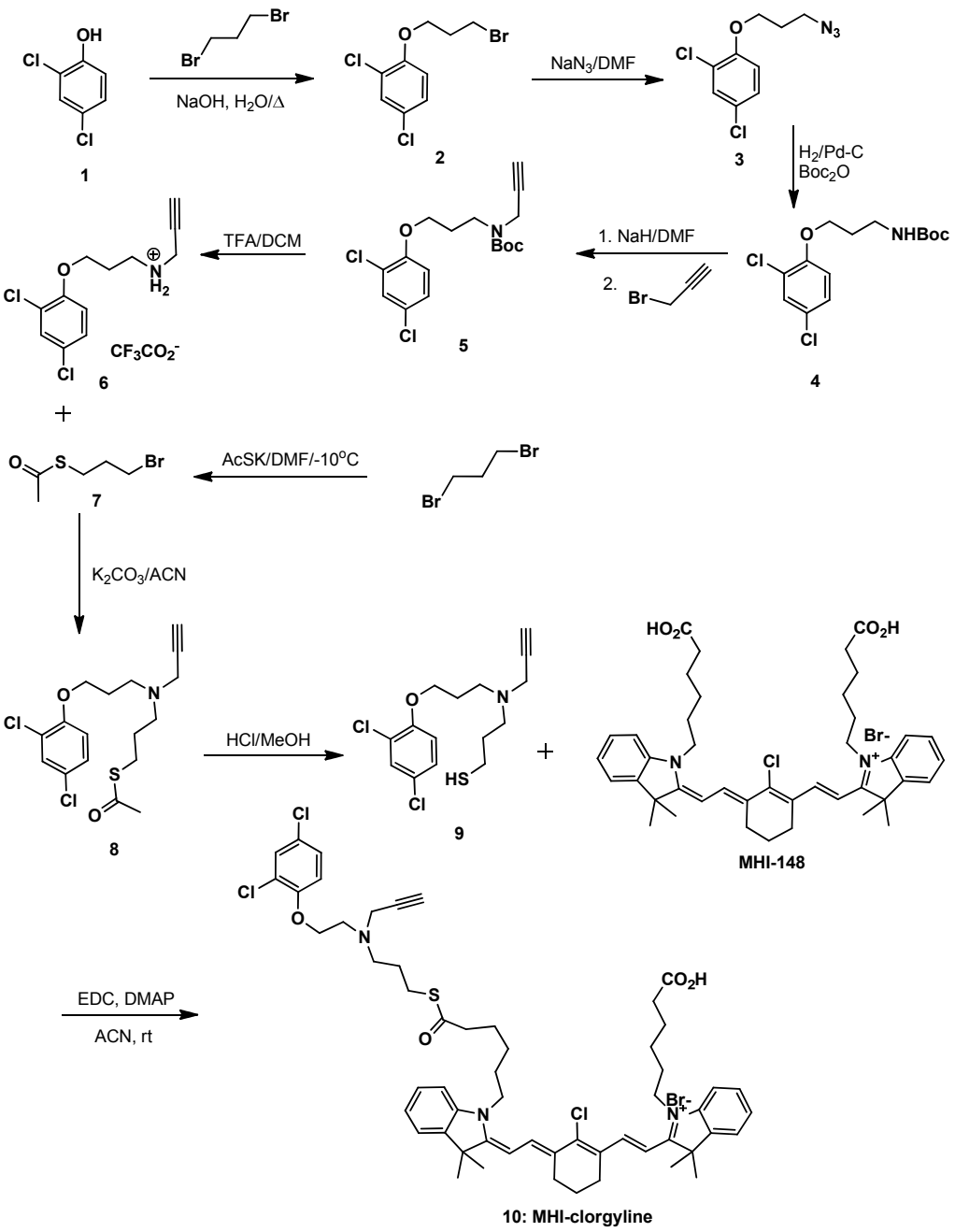

Scheme 1. Synthesis of NIR dye MHI-148 –clorgyline conjugate (MHI-clorgyline).

Preparation of NIR-clorgyline started with commercially available 2,4-dichlorophenol **1**. This compound was alkylated under standard conditions (NaOH, H_2O) with 1,3-dibromopropane. The product **2** was then reacted with NaN_3 in DMF to yield the azide **3**, which was subjected to the next step as a solution in MTBE without further purification. The solution of **3** was hydrogenated under low H_2 pressure using Pd on activated charcoal as a catalyst in the presence of Boc_2O and resulting in the formation of the carbamate **4**. This compound was alkylated with propargyl bromide using NaH in dry DMF, producing Boc-protected alkyne **5**. The Boc protecting group was removed under acidic conditions using TFA in DCM. The product **6** was alkylated again with 1-bromo-3-thioacetylpropane **7**, resulting in the formation of **8**, albeit in low yield. Removal of the acetyl protective group was carried out in methanolic HCl and afforded intermediate **9**. This intermediate was then coupled with MHI-148 dye using EDC and 4-DMAP to afford the product **MHI-clorgyline 10**. This product was purified using reverse-phase HPLC and its identity and purity was confirmed by high-resolution mass spectrometry.

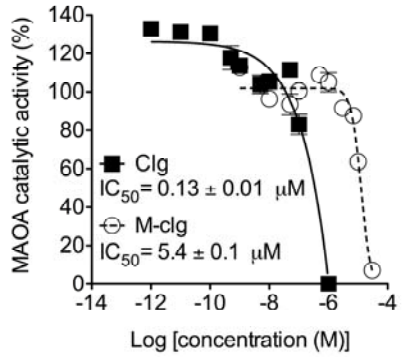

Figure 4. MAOA catalytic activity was determined in LNCaP cells treated with either clorgyline (Clg) or MHI148-clorgyline (M-clg) at indicated concentrations for 24 h.

Task 3b: We determined inhibitory activity of the MHI-clorgyline using MAOA inhibition assays with radiolabeled substrates in LNCaP cell line (Figure 4). In parallel, clorgyline was used as a positive control. MAOA catalytic activity was inhibited by clorgyline at a lower concentration than that of MHI-clorgyline. To test the efficacy of the MHI-clorgyline in inhibiting PCa cell growth we conducted an MTS assay in LNCaP, C4-2B and MAO-overexpressing PC3 cell lines after 96 h of incubation with MHI-clorgyline. Clorgyline was used as a positive control. The results are presented in Figure 5. Remarkably, MHI-clorgyline has shown significantly higher activity as compared to clorgyline.

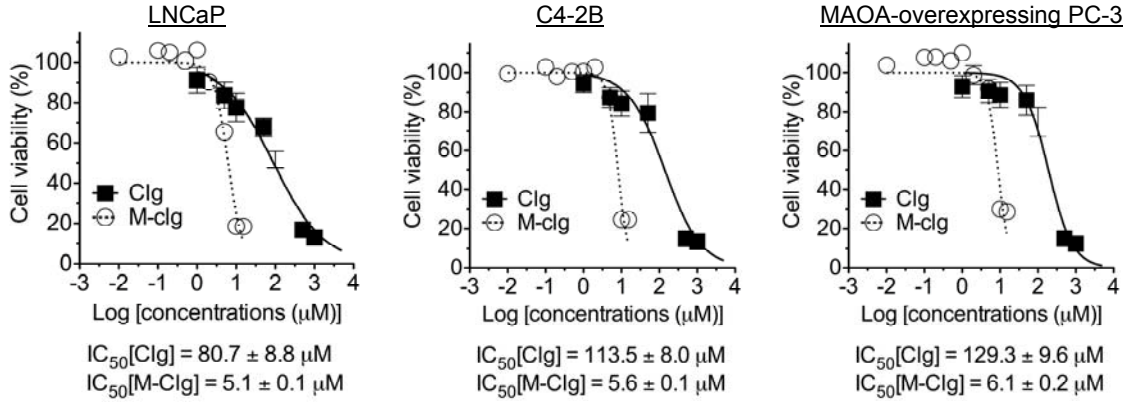

Figure 5. Cell growth inhibition curves for MHI-clorgyline and clorgyline in three PCa cell lines.

We next conducted cell number counting assay in the same cell lines treated with clorgyline and MHI-clorgyline (Figure 6). Again, treatment with MHI-clorgyline was more effective than that of the clorgyline.

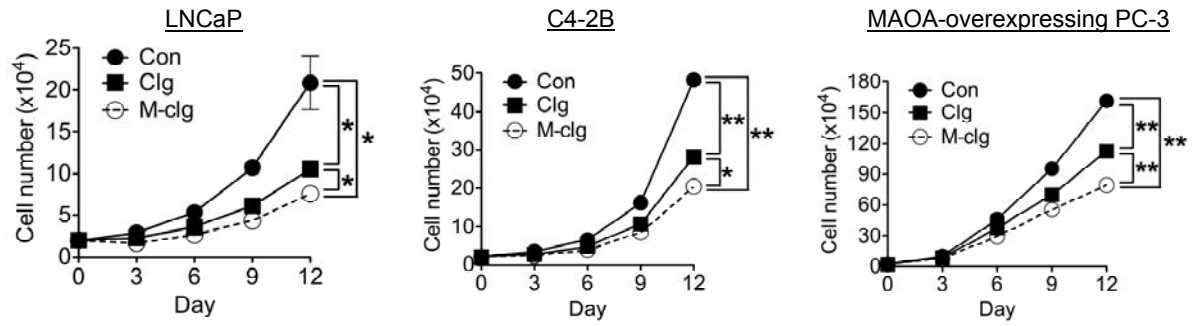

Figure 6. Cell number counting of LNCaP, C4-2B and MAOA overexpressing PC-3 cells treated with 1 μM of clorgyline (clg) or MHI-clorgyline (M-clg) for 12 days consecutively. PBS was used as the vehicle. 2 x 10^4 cells were initially seeded. *, $p<0.05$.

We also tested MHI-clorgyline and clorgyline in LNCaP cells in a standard colony formation assay and compared the results to shRNA treatment (Figure 7). In this assay both MHI-clorgyline and clorgyline showed significant reduction in the colony numbers (~50%) and were more effective than shRNA (~25%).

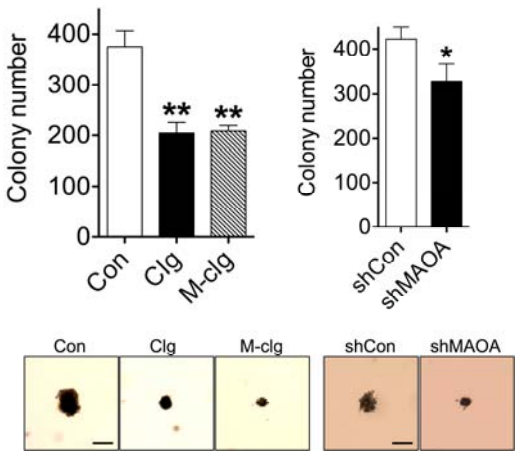

Figure 7. Colony formation assays in LNCaP cells treated with 1 μM clorgyline (clg) or MHI-clorgyline (M-clg) or LNCaP cells targeted by either a scrambled shRNA (shCon) or a MAOA-targeting shRNA (shMAOA). Representative colonies were photographed and shown (left, original magnification, 100x, scale bars represent 50 μm; right, original magnification, 200x, scale bars represent 100 μm). *, $p<0.05$; **, $p<0.01$.

Task 3c: We utilized laser-scanning confocal microscopy (LSCM) to determine the extent of targeting and intracellular localization of the MHI-clorgyline in PCa cells. Heptamethine cyanine dyes, such as MHI-148 and its conjugate MHI-clorgyline emit strong fluorescence in the near-IR region at 820-860 nm upon excitation at 750-780 nm.(*8*) This fluorescence can be used to visualize the intracellular location of the dye or the conjugate. Since MAOA is mitochondria-bound, we anticipate that MHI-clorgyline will also localize there. The compound rapidly accumulated in C4-2B PCa cells and, as expected, localized in the mitochondria, as determined by co-staining cells with mitochondria-specific dye, Mitotracker Green (Figure 8).

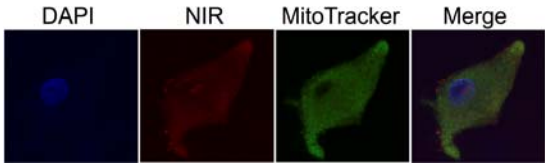

Figure 8. Confocal images of a single LNCaP cell incubated with MHI148-clorgyline. DAPI and MitoTracker agent were used to stain the nucleus and mitochondria of cells, respectively.

4. KEY RESEARCH ACCOMPLISHMENTS:

- We established MAOA-knockdown (KD) PCa cells: LNCaP, C4-2 and $ARCaP_M$.
- We have shown that MAOA effect is driving epithelial-to-mesenchymal transition (EMT) and hypoxia in human prostate cancer xenografts.
- We demonstrated that MAO A knockdown reduces the rate of growth and metastasis of PCa cells.
- We designed an efficient organic synthetic route leading to novel tumor-targeting agent – MHI-clorgyline.
- We showed that MHI-clorgyline targets mitochondria of prostate cancer cells.
- MHI-clorgyline inhibited MAOA activity in PCa cells, resulting in a suppression of cell growth and the rate of colony formation (see project Summary, Figures 6 & 7).

5. CONCLUSION:

During this first year of the grant, we established the role of MAOA in human PCa progression and metastasis. Through our experimental work we began to define the molecular basis of MAOA functions in prostate cancer. We established MAOA knockdown cell lines and tumor xenografts, which allowed us to further define the role of MAOA in prostate cancer progression and metastasis. Furthermore, through the effort of synthetic chemistry, imaging and molecular pharmacology we developed an effective MAOA targeting strategy in tumors as well as means of inhibition of its downstream targets. Our novel MAOA inhibitor, MHI-clorgyline, is selectively delivered to prostate cancer cells using a dye-drug conjugate platform to specifically target tumors without collateral damage to central nervous systems and the impairment of the normal tissue functions. The dye-drug conjugates can be visualized in tumors through the use of near-infrared (NIR) imaging, which could also be utilized as a monitoring tool for the assessment of the drug efficacy, its delivery, and its impact on the tumor growth.

The immediate future plans of this study is in vivo assessment of the efficacy of our dye-drug conjugate in mouse PCa tumor xenografts and further mechanistic study of its action in vivo. The long-term goals are translation of our MAOA inhibitors from bench to bedside for improved treatment of PCa growth and metastasis.

6. PUBLICATIONS, ABSTRACTS, AND PRESENTATIONS:

a.

(1) Lay Press: None

(2) Peer-Reviewed Scientific Journals:
Wu JB, Shao C, Li X, Hu P, Chen Y-T, Li Q, Yin F, Li Y, Zhau HE, Shih JC, and Chung LWK. *"MAO A: a Novel and Effective Therapeutic Target for Prostate Cancer." J. Cancer Invest*. 2013, in Revision.
Invited Articles: Shih, J. C., "Translation Research in Autism and Cancer: Novel Roles of MAO." in *Catecholamine Research in the 21st Century: Summary of the 10th International Catecholamine Symposium*, 2012, Eiden, L.E., ed.

(3) Abstracts:
Shih, J.C., Wu, J.B., Bortolato, M., Chen, K. *"Translation Research in Autism and Cancer: Novel Roles of MAO"* at *the 15th International Amine Oxidase Workshop*, Toulouse, France, 2012.

b. Presentations and posters made during the last year:

Shih, J.C., Wu, J.B., Bortolato, M., Chen, K. *"Translation Research in Autism and Cancer: Novel Roles of MAO"* at *the 15th International Amine Oxidase Workshop*, Toulouse, France, 2012.

Invited Talk: Shih, J.C., "*Novel Role of MAO A in Prostate Cancer Progression."* International Research Collaboration Workshop, Taipei, Taiwan, 2012.

Seminars:
Shih, J. C., *"Novel Role of MAO A in Prostate Cancer Progression."*
Taipei Medical University, 2012
National Yang-Ming University, 2013
Academia Sinica, Taipei, Taiwan, 2013

Posters:
Wu JB, Hu P, Shao C, Zhau HE, and Chung LW. (2012). *"Monoamine oxidase A confers prostate cancer EMT by stabilizing HIF1α and enhancing VEGF-mediateCond Twsit1 activation."* at *the 4th Annual Cancer Institute Research Poster Presentation*. Cedars-Sinai Medical Center, Los Angeles, CA.

Wu, J.B., Shao, C., Li, X., Hu, P., Chen, Y.T., Dou, X., Sahu, D., Li, W., Harada, H., Wang, R., Zhau, H.E. & Chung, L.W. (2013). *"Hypoxia-mediated cancer imaging by*

a novel class of near-infrared (NIR) heptamethine cyanine dyes." at *the 104th American Association for Cancer Research Annual Meeting*. Washington, DC.

7. INVENTIONS, PATENTS AND LICENSES: 1 Patent Application

Inventors: Shih J.C., Olenyuk B., Wu, B., Chung, L.W.K., Zhau, H.
Invention Title: Monoamine Oxidase Inhibitors and Methods for Treatment and Diagnosis of Prostate Cancer
Patent Application Number: PCT/US2012/048407
Filing Date: Jul 26, 2012
Publication Number: WO2013016580 A3
Publication Date: Mar 28, 2013

8. REPORTABLE OUTCOMES:

None.

9. OTHER ACHIEVEMENTS:

Facilitated US-Taiwan International Student Exchange
Trained PhD Candidates in Pharmaceutical Sciences

10. REFERENCES:

1. M. Bortolato, K. Chen, J. C. Shih, Monoamine oxidase inactivation: from pathophysiology to therapeutics. *Adv Drug Deliv Rev* **60**, 1527 (Oct-Nov, 2008).
2. J. C. Shih, K. Chen, M. J. Ridd, Monoamine oxidase: from genes to behavior. *Annu Rev Neurosci* **22**, 197 (1999).
3. S. Josson *et al.*, beta2-microglobulin induces epithelial to mesenchymal transition and confers cancer lethality and bone metastasis in human cancer cells. *Cancer Res* **71**, 2600 (Apr 1).
4. S. Y. Sung *et al.*, Coevolution of prostate cancer and bone stroma in three-dimensional coculture: implications for cancer growth and metastasis. *Cancer Res* **68**, 9996 (Dec 1, 2008).
5. D. Trachootham, J. Alexandre, P. Huang, Targeting cancer cells by ROS-mediated mechanisms: a radical therapeutic approach? *Nat Rev Drug Discov* **8**, 579 (Jul, 2009).
6. V. Flamand, H. Zhao, D. M. Peehl, Targeting monoamine oxidase A in advanced prostate cancer. *J Cancer Res Clin Oncol* **136**, 1761 (Nov).
7. L. True *et al.*, A molecular correlate to the Gleason grading system for prostate adenocarcinoma. *Proc Natl Acad Sci U S A* **103**, 10991 (Jul 18, 2006).

8. X. Yang *et al.*, Near IR heptamethine cyanine dye-mediated cancer imaging. *Clin Cancer Res* **16**, 2833 (May 15).
9. H. Y. Zhau *et al.*, Androgen-repressed phenotype in human prostate cancer. *Proc Natl Acad Sci U S A* **93**, 15152 (Dec 24, 1996).
10. L. De Colibus *et al.*, Three-dimensional structure of human monoamine oxidase A (MAO A): relation to the structures of rat MAO A and human MAO B. *Proc Natl Acad Sci U S A* **102**, 12684 (Sep 6, 2005).

11. APPENDICES:

Copy of an Article:
Wu JB, Shao C, Li X, Hu P, Chen Y-T, Li Q, Yin F, Li Y, Zhau HE, Shih JC, and Chung LWK. *"MAO A: a Novel and Effective Therapeutic Target for Prostate Cancer." J. Cancer Invest*. 2013, in Revision.

MAOA: a novel and effective therapeutic target for prostate cancer

Jason Boyang Wu[1], Chen Shao[1, 2], Xiangyan Li[1], Peizhen Hu[1, 3], Yi-Ting Chen[1], Qinlong Li [1,3], Fei Yin[4], Yang Li[4], Haiyen E. Zhau[1], Jean C. Shih[4], and Leland W. K. Chung[1]

[1]Uro-Oncology Research Program, Department of Medicine, Cedars-Sinai Medical Center, Los Angeles, CA 90048, U.S.A.

[2]Department of Urology, Xijing Hospital, Fourth Military Medical University, Xi'an, Shaanxi 710032, China

[3]Department of Pathology, Xijing Hospital, Fourth Military Medical University, Xi'an, Shaanxi 710032, China

[4]Deparment of Pharmacology and Pharmaceutical Sciences, School of Pharmacy, University of Southern California, Los Angeles, CA 90089, U.S.A.

Address correspondence to: Leland W. K. Chung, Ph.D., Cedars-Sinai Medical Center, 8750 Beverly Blvd., Atrium 103, Los Angeles, CA 90048, USA. Phone: 310.423.7622; Fax: 310.423.8543; E-mail: Leland.Chung@cshs.org (L.W-K. Chung). Or Jean C. Shih, Ph.D., University of Southern California, 1985 Zonal Ave., PSC 518, Los Angeles, CA 90089, U.S.A. Phone: 323.442.1441; Fax: 323.442.3229; E-mail: jcshih@usc.edu (J.C. Shih).

Abstract

High-grade aggressive prostate cancer (PCa) exhibits increased monoamine oxidase A (MAOA) expression, a mitochondrial enzyme that degrades monoamine neurotransmitters and dietary amines. However, the functional roles of MAOA and its molecular basis in PCa remain unclear. We show that MAOA assumes a key function by inducing epithelial-to-mesenchymal transition (EMT) and stabilizing HIF1α, a transcription factor that mediates hypoxia through an elevation of reactive oxygen species (ROS) in PCa, coordinately enhancing the growth and invasiveness of PCa cells. Mechanistic studies indicated that MAOA activates VEGF and its co-receptor Neuropilin-1 and drives EMT by stimulating Akt/FoxO1/Twist1 signaling through a novel FoxO1-binding site in *Twist1* promoter. Importantly, this mechanism is manifested in high-grade PCa specimens. Targeted knockdown of MAOA via shRNA reduced or even eliminated prostate tumor growth in both syngeneic and immune-compromised mouse xenograft models. Finally, we found that high MAOA expression correlated with worse clinical outcomes in PCa patients. Together, these findings define the molecular basis of MAOA in PCa pathogenesis and provide a rationale for the pursuit of MAOA as a highly effective therapeutic target for PCa therapy.

Introduction

Prostate cancer (PCa) is the second leading cause of male cancer death in the Western world (1). It can be clinically categorized into different risk groups primarily based on histological grade (Gleason score), clinical TNM stage, and the levels of serum prostate-specific antigen (PSA) (2). Aggressive, poorly differentiated high-grade PCa is incurable and potentially lethal, which drives the need for greater understanding of the molecular basis of PCa progression for improved opportunities to eliminate the lethal phenotype of PCa.

Monoamine oxidase A (MAOA) is a mitochondria-bound enzyme that catalyzes the degradation of monoamine neurotransmitters and dietary amines by oxidative deamination, which produces a by-product, hydrogen peroxide, a major source of reactive oxygen species (ROS) (3-5). ROS can predispose cancer cells to DNA damage and cause tumor initiation and progression (6). In the last several decades, MAOA has been widely studied in the context of neuropsychiatric disorders, such as aggressive behaviors and mental depression (5). Recently, a significant correlation was established between increased levels of MAOA expression and high Gleason grade or poorly differentiated human prostate tumors (7, 8). MAOA is exclusively expressed in the epithelial cells of prostatic glands with undetectable levels in stromal counterparts. These observations collectively suggest that MAOA may function in an autocrine manner to regulate the proliferation and differentiation of prostatic epithelial cells (9).

Prostate tumorigenesis and cancer development are regulated by several oncogenic cues leading to dysregulated growth, increased stemness and plasticity by which cancer cells acquire increased migratory, invasive and metastatic potential through epithelial-to-mesenchymal transition (EMT) (10). Evidence also supports the ability of cancer cells to adapt a hypoxia-inducible factor 1α (HIF1α) pathway to resist oxidative stress, which cooperatively promotes an increasingly aggressive phenotype in cancer cells (11, 12).

In this study, we proposed that increased MAOA expression in high-grade PCa may be an important contributor to its dysregulated growth and de-differentiation of the glandular epithelial phenotype. We demonstrated the ability of MAOA to induce morphological transformation, invasion and proliferation of PCa cells. Moreover, genetic targeting of MAOA using shRNA effectively inhibited or even completely eliminated prostate tumorigenesis in mouse xenograft models. Mechanistically, we showed that MAOA potentiated aggressive PCa behavior by converging functional interplay among EMT, hypoxia and oxidative stress. Additionally, evidence for MAOA function in PCa also extended to human clinical PCa specimens. These findings establish MAOA as a viable therapeutic target in PCa and provide a rationale for the development of MAOA-targeted therapies.

Results

MAOA Suppresses Epithelial Phenotype and Promotes Mesenchymal Transition. Although MAOA expression has been previously demonstrated in human PCa tissues (7), its concurrent expression with the differential expression of EMT pathways has not been pursued. In a series of clinical specimens, we observed consistently that high Gleason grade 5 PCa is distinguished from low grade 3 PCa by characteristic morphologic features such as the merger of neoplastic glands and cytological de-differentiation (13). Higher Gleason grade tumors also expressed diminished levels of E-cadherin (an epithelial marker) and increased expression of Vimentin (a mesenchymal marker) and MAOA in the same clinical specimens (Figure 1A). These results suggest that high Gleason grade cancers exhibit EMT characteristics associated with increased MAOA expression and aggressive behaviors, which led us to hypothesize that MAOA may regulate EMT in PCa.

To address this hypothesis, we used human PCa cell lines, PC-3 and LNCaP, as models since these cell lines express either low (PC-3) or high (LNCaP) basal levels of MAOA (14). Stably enforced expression of a MAOA expression construct in PC-3 cells resulted in the transition to a dispersed, fusiform morphology, a significant loss of E-cadherin and increased expression of Vimentin, N-cadherin and Twist1 (Figure 1B). To establish that MAOA regulates *E-cadherin* transcription, we assayed the activity of *E-cadherin* promoter hooked with a luciferase reporter gene in PC-3 cells that stably expressed either an empty vector or a MAOA construct. As shown in Figure 1C, MAOA-overexpressing cells displayed substantially diminished promoter activity compared to control cells. By contrast, stable knockdown of MAOA in LNCaP cells with a MAOA-targeting shRNA (shMAOA) increased expression of E-cadherin and reduced levels of Vimentin and N-cadherin compared to control cells delivered with a scramble shRNA (shCon) (Figure 1D). Moreover, overexpression of MAOA also led to a significant

increase in migration and invasion of PC-3 cells, a characteristic function of EMT. In contrast, knockdown of MAOA in LNCaP cells reduced the ability of cells to migrate or invade (Figures 1E and 1F). In addition, stable knockdown of MAOA in two other human PCa cell lines, C4-2 and $ARCaP_M$, also markedly attenuated mesenchymal features by changes in cell morphology, reduced mesenchymal markers and cell migratory and invasive behaviors (Supplemental Figure 1). These data provide further evidence that MAOA can drive the transition of PCa cells toward a mesenchymal state, which can be reversed when MAOA is genetically knocked down.

MAOA Stabilizes HIF1α via ROS Generation and PHD Destruction. Hypoxia, a common condition found in a wide range of solid tumors including PCa, is often associated with poor prognosis and frequent expression of an aggressive phenotype promoted by EMT (15). HIF1α, a master regulator of hypoxia, mediates hypoxic effects by activating relevant downstream target genes involved in many aspects of tumor progression, such as increased tumor glycolysis, angiogenesis, invasion, migration and metastasis (15, 16). Since increased MAOA expression promotes EMT, we assessed a possible relationship between MAOA and HIF1α.

This possibility was evaluated first by investigating whether MAOA directly regulates HIF1α stability under normoxic conditions. In the presence of high oxygen, HIF1α is rapidly degraded, which prevents a direct measurement in whole-cell lysates, but HIF1α is detectable from isolated nuclei. As shown in Figure 2A, nuclei isolated from MAOA-overexpressing PC-3 cells during normoxia revealed elevated levels of HIF1α relative to the vector-expressing control cells. Likewise, when these cells were cultured under hypoxic conditions at 1% O_2, HIF1α was stabilized earlier and to a higher degree in MAOA-overexpressing cells compared to control cells in whole-cell lysates (Figure 2B). Moreover, the HIF1α target genes, including EMT-promoting genes, *Snail2* and *Twist1*, vascular endothelial growth factor A (*VEGF-A*), and glucose transporter 1 (*Glut1*), were

significantly upregulated in MAOA-overexpressing cells compared to control cells during hypoxia. Enforced expression of MAOA and hypoxia further showed additive effects on the expression of HIF1α target genes (Figure 2C). To test whether the loss of MAOA directly represses HIF1α, we examined the levels of HIF1α and its target genes in LNCaP cells with stable knockdown of MAOA. MAOA knockdown resulted in reduced HIF1α stabilization in hypoxic cells (Figure 2D). Moreover, the induction of *Snail2*, *Twist1*, *VEGF-A* and *Glut1* during hypoxia was suppressed by MAOA knockdown, indicating that MAOA is required for HIF1α function (Figure 2E). Notably, *HIF1α* mRNA levels were not affected by differential MAOA expression (Figures 2C and 2E), suggesting that MAOA may regulate HIF1α stability via translational or post-translational modifications. These data in aggregate suggest that MAOA modulates the stabilization of HIF1α and the induction of crucial HIF1α target genes that coordinate cancer progression.

The regulation of HIF1α is complex and has not been fully understood. During normoxia, HIF1α is hydroxylated at two proline residues by a family of oxygen-dependent prolyl hydroxylases (PHD1-3), which enables the tumor suppressor von Hippel-Lindau (vHL) to bind and target HIF1α for ubiquitination and proteasomal degradation (16). Since *HIF1α* mRNA levels remained unchanged by MAOA expression (Figures 2C and 2E), we tested whether MAOA exerted a post-translational effect on HIF1α protein stability. We ruled out the direct interaction between these two proteins given their distinct cellular localization in the hypoxic state. MAOA appears in the outer membrane of mitochondria to execute enzymatic reactions, whereas HIF1α, when activated, functions as a nuclear transcription factor.

We next measured the extent of HIF1α hydroxylation to test the hypothesis that MAOA regulates HIF1α stability by affecting PHD activity directly. We determined PHD activity in control and MAOA-overexpressing PC-3 cells by treating cells with the proteasomal inhibitor MG132 to prevent hydroxylated HIF1α from being degraded. As

shown in Figure 3A, more HIF1α but significantly less hydroxylated HIF1α accumulated during MG132 treatment in MAOA-overexpressing cells, suggesting lower PHD activity in the presence of MAOA.

To further validate that MAOA regulates HIF1α through the PHDs, we determined the effect of dimethyloxalylglycine (DMOG) treatment, a potent PHD inhibitor, on HIF1α stability and the expression of HIF1α target genes in MAOA-overexpressing PC-3 cells. If MAOA affects HIF1α stability by modulating PHD activity, DMOG treatment should blunt the effects of MAOA overexpression and produce equivalent levels of HIF1α activity in control and MAOA-overexpressing cells. As shown in Figure 3E, the control and MAOA-overexpressing cells demonstrated equal levels of HIF1α stabilized in response to DMOG treatment (lane 3 vs. lane 7). These results are consistent with the subsequent observation that induction of HIF1α by MAOA resides in the depressed PHD activity, hence HIF1α was stabilized by DMOG treatment to a lesser extent in MAOA-overexpressing cells (Figure 3B). During hypoxia, HIF1α target genes such as *VEGF-A* and *Glut1* were induced more robustly when MAOA was overexpressed in cells (Figure 2C), which was blunted by DMOG treatment (Figure 3B). These data are consistent with a model in which overexpression of MAOA reduced PHD activity thereby rendering PHD less responsive to DMOG inhibition, resulting in a smaller change in PHD activity and less induction of HIF1α target genes in MAOA-overexpressing cells. Taken together, our results suggest that MAOA-overexpressing PCa cells had reduced PHD activity and enhanced HIF1α activity and downstream target gene expression.

In addition to intracellular oxygen concentration, PHD activity can also be regulated by several intracellular signals including ROS, which has been shown to inhibit the PHDs and stabilize HIF1α (16-18). Moreover, hypoxia enhances ROS production, a seemingly required step for the hypoxic activation of HIF1α (19, 20). Because MAOA-mediated enzymatic reactions produce hydrogen peroxide, a major form of ROS, as a by-product,

we hypothesized that increased ROS in MAOA-overexpressing cells could contribute to the inhibition of PHDs and stabilization of HIF1α in PCa cells (16-18). We showed that overexpression of MAOA increased either mitochondrial hydrogen peroxide or general ROS generation in PC-3 cells, while these ROS levels were reduced in MAOA-knockdown LNCaP cells (Supplemental Figure 2). Next, we found that hypoxia triggered a significantly higher increase in ROS production in MAOA-overexpressing cells than control cells (Figure 3C), providing a mechanistic explanation for why MAOA-overexpressing cells have exaggerated responses to hypoxia.

Next, we treated cells with the antioxidant N-acetylcysteine (NAC) to suppress ROS and hence block the downstream effects of MAOA overexpression mediated by intracellular ROS. Indeed, the higher levels of HIF1α under hypoxia in MAOA-overexpressing cells could be significantly attenuated by NAC treatment (Figure 3D). Moreover, when PHD activity was blocked by DMOG treatment, both control and MAOA-overexpressing cells demonstrated comparable levels of HIF1α, in which NAC failed to destabilize HIF1α (Figure 3E). Consistent with decreased HIF1α expression in NAC-treated MAOA-overexpressing cells (Figure 3D), the expression of HIF1α target genes, *VEGF-A*, *Glut1* and *Twist1*, were reduced to control levels in NAC-treated MAOA-overexpressing cells (Figure 3F). To test whether increased ROS contributes to the proliferation of MAOA-overexpressing cells, we determined the growth profiles in cells cultured with NAC. Strikingly, we observed that NAC blunted the enhanced proliferation of MAOA-overexpressing cells, restoring their growth rates to that of the control cells (Figure 3G). MAOA regulation of ROS consequently augmented hypoxic responses by increasing the steady-state levels of HIF1α and the expression of its target genes, *VEGF-A*, *Glut1* and *Twist1*, converging the cell signaling network toward increased mesenchymal transition and enhanced cell proliferation in MAOA-overexpressing cells (Figure 3H).

MAOA Activates VEGF-A/Neuropilin-1 Signaling and Its Downstream Akt/FoxO1 Pathway. Since hypoxia reportedly can affect cell behavior by promoting EMT, we hypothesized that the HIF1α target gene *VEGF-A* plays a crucial mediator role in controlling the downstream signaling for the MAOA-driven EMT and its associated increased aggressive phenotype in PCa cells. VEGF has been implicated in poor prognosis and survival in PCa patients, and an elevated level of VEGF could be the trigger for an angiogenic switch in the lethal progression of advanced PCa (21). To test this hypothesis, we assessed *VEGF-A* expression by qRT-PCR in control and MAOA-overexpressing PC-3 or in control and MAOA-knockdown LNCaP cells, and observed that overexpression of MAOA significantly increased *VEGF-A* expression (Figure 4A). We quantified VEGF-A expression in the culture media of MAOA-manipulated PCa cells by ELISA and confirmed that MAOA up-regulates VEGF-A expression and its extracellular secretion (Figure 4A).

To elucidate the mechanism by which MAOA activation of VEGF-A mediates downstream signaling to promote EMT, PC-3 cells were treated with recombinant $VEGF_{165}$ and select protein kinase pathways were examined. As shown in Figure 4B, there was a significant increase in the relative phosphorylation of both Akt and its downstream target FoxO1 as assessed by immunoblotting. Akt plays a central role by activating its many downstream target genes in regulating PCa development and progression (22). FoxO1, a member of the O subclass of the forkhead family of transcription factors, can be regulated via the phosphorylation of Akt upon PI3K/Akt signaling activation, and has demonstrated the pro-apoptotic function in a variety of cancers (23). We further showed that Akt/FoxO1 signaling was activated in MAOA-overexpressing PC-3 cells, and conversely attenuated Akt/FoxO1 activity was observed in MAOA-knockdown LNCaP cells (Figure 4C), suggesting that this signaling pathway is downstream of MAOA.

Autocrine VEGF signaling in tumor cells occurs through a non-angiogenic cell proliferative mechanism via increased autocrine VEGF-A and its co-receptor, Neuropilin-1 (NRP1) interaction. This interaction has been implicated in cancer cell autonomy and aggressive behaviors (24). Given that NRP1 can regulate Akt activity (25), we examined autocrine VEGF-NRP1-mediated signaling and evaluated the relationship between MAOA and Akt/FoxO1 in PC-3 cells with stable NRP1 knockdown using a lentiviral shRNA approach. As shown in Figure 4D, diminished NRP1 expression reduced the phosphorylation of both Akt and FoxO1 in PC-3 cells. Strikingly, overexpression of MAOA significantly enhanced NRP1 expression and increased the phosphorylation of Akt and FoxO1, which was reduced by genetic knockdown of NRP1. Moreover, we uncovered the role of MAOA in facilitating the nuclear export of FoxO1 to cytoplasm. As shown in Figure 4E, either MAOA overexpression or treatment with recombinant $VEGF_{165}$ decreased FoxO1 expression in the nucleus but increased its activity in the cytoplasmic fraction, using Lamin B1 and GAPDH as the nuclear and cytoplasmic markers, respectively. Conversely, genetic knockdown of NRP1 increased nuclear but decreased cytoplasmic FoxO1 activity. Similar results were obtained with control and MAOA-overexpressing PC-3 tumor xenografts (Supplemental Figure 3), and the activation of HIF1α/VEGF-A/NRP1 signaling by MAOA overexpression was demonstrated by immunohistochemical (IHC) analyses (Figure 4F). Knockdown of NRP1 resulted in a significant decrease of MAOA-induced migration and invasion in PC-3 cells (Figure 4G). Likewise, NRP1 knockdown also dramatically reduced the cell proliferation rate in MAOA-overexpressing PCa cells to a level lower than that of the controls (Figure 4H). Taken together, these functional characteristics indicate that the VEGF-A/NRP1 signaling pathway may mediate MAOA-driven EMT and cell proliferation via the downstream mitogenic Akt/FoxO1 pathway.

Twist1 Expression Is Directly Regulated by Transcription Factor FoxO1. We screened a spectrum of key transcription factors known to promote EMT under regulation by MAOA, and identified Twist1 as the downstream target of MAOA (Figure 1). Twist1, a basic helix-loop-helix (bHLH) transcription factor, is a master regulator of EMT, and its expression in tumors often correlates with aggressive disease and poor outcome (26, 27). To assess the potential regulation of Twist1 by MAOA, we determined both *Twist1* mRNA and its promoter activity in PCa cells with manipulated MAOA expression. As shown in Figure 5A, overexpression of MAOA increased *Twist1* mRNA and promoter activity in PC-3 cells, whereas these Twist1-related activities were reduced upon MAOA knockdown in LNCaP cells, suggesting that MAOA may regulate *Twist1* at the transcriptional level.

Akt drives EMT and cancer development by regulating many downstream target genes including Twist1 (28, 29), but specific Akt-responsive signaling pathway(s) that regulates Twist1 remains to be clarified. The transcription factor forkhead box (Fox) proteins capable of being phosphorylated by Akt play a dominant role in cancer development and progression (30, 31). Moreover, Fox proteins have been demonstrated to regulate EMT, which led us to speculate that FoxO1 may directly regulate Twist1. Since Fox proteins were shown to regulate EMT-inducing factors (32), we determined if FoxO1 can regulate Twist in PC-3 cells. We established stable PC-3 cells that overexpressed a constitutively active *FoxO1* expression construct (AAA *FoxO1*) with three mutated phosphorylation sites (T24A, S256A and S319A). AAA FoxO1 is sequestered in the nucleus without degradation (33). As shown in Figure 5B, enforced expression of AAA FoxO1 significantly reduced Twist1 protein expression, whereas stable shRNA-mediated silencing of FoxO1 increased Twist1 levels in PC-3 cells, suggesting a negative regulatory link between these two proteins. Considering the innate feature of FoxO1 as a transcription factor, we further determined whether FoxO1

transcriptionally regulates *Twist1* expression, and we showed a reproducible negative regulation of *Twist1* mRNA by FoxO1 in PC-3 cells (Figure 5C). To explore the possible direct influence of FoxO1 on the promoter of *Twist1* gene, a 1-kb DNA segment located upstream of the transcription initiation site of *Twist1* was introduced as a luciferase reporter construct into PC-3 cells (34). Since FoxO1 can affect the transcription of target genes either through direct binding to their consensus DNA sequences in the promoter or via indirect protein-protein interactions with other transcription factors or cofactors (35), we distinguished these two alternative mechanisms by using a *FoxO1* mutant (AAA FoxO1 H215R) that is deficient in DNA binding. As shown in Figure 5D (left panel), in contrast to its wild-type (WT) counterpart, which strongly repressed *Twist1* promoter activity, the *FoxO1* mutant failed to do so. Hence, the action of FoxO1 on the *Twist1* promoter appeared to require the intact DNA-binding activity of FoxO1. This regulation is further supported by the observation that knockdown of FoxO1 increased *Twist1* promoter activity in PC-3 cells (Figure 5D, right panel).

It remained unclear whether the observed repression is mediated by direct binding of FoxO1 to the *Twist1* promoter. To address this issue, we attempted to identify a FoxO1-response element in the *Twist1* promoter. Serial deletion of the *Twist1* promoter combined with sequence analysis revealed a region within the *Twist1* promoter (-56/-50) that exhibits strong sequence similarity to the canonical AT-rich FoxO1-binding site (Figure 5E, upper panel) (36, 37). To test whether the potential direct regulation of *Twist1* by FoxO1 is conserved throughout evolution, we searched for the consensus FoxO1-binding site and its surrounding sequences in the human *Twist1* promoter across species. Interestingly, we found that this element (CCAAACT) is highly conserved among amniotic genomes examined, including chimpanzee, mice, rats and cows (Figure 5E, lower panel). Accordingly, we generated a mutant *Twist1* promoter reporter construct harboring three point mutations in the center of the putative FoxO1-response

element. As shown in Figure 5F, the resulting mutant *Twist1* promoter was no longer repressed by ectopic expression of FoxO1 in PC-3 cells. This mutant *Twist1* promoter reporter construct was further introduced into MAOA-overexpressing PC-3 cells, and in contrast to its WT counterpart, the mutant did not respond to MAOA overexpression (Figure 5G). To confirm the direct occupancy of FoxO1 with the sequences in the *Twist1* promoter *in vivo*, we extended these studies by performing chromatin immunoprecipitation (ChIP) analysis. We undertook chromatin complex immunoprecipitated with anti-FoxO1 antibody from both control and MAOA-overexpressing PC-3 cells, and analyzed them by qPCR using primers that specifically encompass the putative FoxO1-response element in the *Twist1* promoter. As shown in Figure 5H, we were able to detect the physical association of FoxO1 with the *Twist1* promoter sequences, and such association was reduced in the presence of MAOA overexpression, which is consistent with the observation of less nuclear FoxO1 expression in MAOA-overexpressing PC-3 cells (Figure 4E). Moreover, limited signals were detected from the negative controls whereby either non-specific IgG antibody was used in the immunoprecipitation step or the *Twsit1* exon 1 was probed in order to confirm the targeting specificity of the primer set used in PCR. These results provide evidence that MAOA mediates *Twist1* gene activation via direct interaction of FoxO1 with a specific element located in the *Twist1* promoter.

MAOA Function in Prostate Tumorigenesis and Cancer Progression. The effects of MAOA in promoting EMT, hypoxia and ROS production as described above shed light on how MAOA supports PCa growth and development. To test this hypothesis, we established multiple prostate tumor xenograft mouse models to validate the functional roles of MAOA. We used 3 human PCa cell lines that show different MAOA expression levels, aggressiveness and invasiveness as well as other innate features such as responses to androgen (38, 39). Considering the importance of the immune system in

PCa growth and progression, we also extended our analysis by using a highly tumorigenic mouse prostate carcinoma MPC3 cell line in an immunocompetent mouse model. The MPC3 line was derived from mouse primary prostate tumors harboring double loss of Pten and Tp53 tumor suppressors. To analyze MAOA function in these tumor xenograft models, we first infected these cells with lentiviral constructs expressing shRNAs directed against the mRNA encoding MAOA, or as a control that targets no known mammalian genes. As indicated in Supplemental Figure 4A, stable introduction of MAOA-specific shRNAs decreased MAOA enzymatic activity by more than 50-70% in all cell lines. As expected, cells expressing MAOA shRNAs had consistently reduced cell proliferation rates in comparison to control cells (Supplemental Figure 4B).

After being subcutaneously implanted into male nude mice, LNCaP and C4-2 cells expressing MAOA shRNAs showed slower tumor growth and formed fewer tumors than the control cells. Those that did form tumors in cells stably expressing MAOA shRNAs were quite small with an average tumor weight of 221 ± 36 mg and 132 ± 81 mg for LNCaP and C4-2 tumors, respectively, compared to larger tumors with an average weight 653 ± 232 mg and 888 ± 632 mg for LNCaP and C4-2 control tumors, respectively (Figure 6A). Strikingly, stable knockdown of MAOA in $ARCaP_M$ and MPC3 cells completely eliminated their *in vivo* growth, in sharp contrast to the expected explosive tumor growth in mice inoculated with the control cells.

As a comparison, we next analyzed the protein expression patterns of select markers in tumor specimens from LNCaP and C4-2 tumor xenografts by IHC. As shown in Figure 6B, Ki-67 staining of tumor specimens revealed a 40-70% decrease of Ki-67^+ cells (Figure 6C) in the MAOA-knockdown group of both LNCaP and C4-2 tumors. MAOA protein staining also showed decreased intensity in MAOA-knockdown tumor specimens for both lines, which is consistent with the results of reduced MAOA enzymatic activity in harvested tumors expressing MAOA shRNAs (Figure 6D), supporting the concept that

genetically silencing *MAOA* gene expression by a shRNA-mediated protocol is highly effective and sustainable under *in vivo* conditions. Moreover, MAOA-knockdown tumor xenografts showed EMT reversal by increased staining of E-cadherin as well as reduced expression of Vimentin, and tumor hypoxia was also repressed, as reflected by less nuclear HIF1α and VEGF-A staining in tumor specimens that expressed MAOA shRNAs (Figure 6B and Supplemental Figure 5). These data from *in vivo* tumor xenograft models provide further evidence that MAOA drives EMT and augments hypoxia.

To examine the contribution of ROS to altered tumor growth *in vivo*, we determined the relevant ROS levels in tumors formed from both control and MAOA-knockdown tumors. MAOA is located in the outer membrane of mitochondria and directly engaged in hydrogen peroxide production via the oxidative deamination of its substrates, which can be subsequently converted into other forms of ROS. We determined the rate of hydrogen peroxide generation in intact tumor mitochondria, which represents specifically the difference in MAOA-originated ROS production, from both control and MAOA-knockdown tumors. As shown in Figure 6E, LNCaP and C4-2 tumors that expressed MAOA shRNAs showed slower rates of hydrogen peroxide generation in comparison to control tumors, suggesting that increased ROS production could be a crucial factor underlying MAOA's role in PCa development as reflected in *in vitro* studies. These data collectively demonstrate that MAOA is a key determinant for tumor growth in mice by coordinating the regulation of EMT, hypoxia and oxidative stress.

The HIF1α/VEGF/FoxO1/Twist1 Pathway Is Manifested in High Gleason Grade PCa. A critical question that arises from our *in vivo* data is whether the expressions of HIF1α, VEGF-A, pFoxO1/FoxO1 and the activation of Twist1 correlate with clinical grading in human PCa, and whether the expressions of these proteins correlate with MAOA in the same specimens as predicted by our hypothesis. To address this question, we used a semiquantitative analysis of IHC staining to assess expressions of these proteins in

specimens from 30 PCa patients, of which 15 were Gleason grade 3 and 15 were grade 5. Expression of MAOA was significantly higher in the cytoplasm of grade 5 compared to grade 3 PCa (Figure 7A), confirming previous studies. We observed intense widespread nuclear HIF1α expression in grade 5 cells that was absent in grade 3 cells. Intense VEGF-A immunostaining was also evident in Gleason grade 5 tumor cells compared to grade 3 tumor cells (Figure 7A).

FoxO1 expression was observed in both the nucleus and cytoplasm, and there was a significant decrease of nuclear expression of FoxO1 in grade 5 tumor cells compared with grade 3 cells. pFoxO1 expression was present in both the nucleus and cytoplasm as well, but predominantly in cytoplasm. Cytoplasmic pFoxO1 showed higher staining in grade 5 cells in contrast to grade 3 cells. The differences seen in FoxO1/pFoxO1 expression patterns between Gleason grade 3 and grade 5 tumors indicate a dynamic nuclear exclusion of FoxO1 with disease progression. Moreover, intense widespread nuclear Twist1 staining was evident in the majority of grade 5 tumor cells concurrently accompanied by a decline of nuclear FoxO1 expression (Figure 7A). These results are consistent with the hypothesis that MAOA increases Twist1 expression by facilitating the phosphorylation and nuclear export of FoxO1 to activate the *Twist1* transcription. These IHC differences were all further confirmed by semiquantitative analysis of multiple specimens (Figure 7B).

Increased MAOA Expression Is Associated with Poor Prognosis in PCa Patients. To determine whether high MAOA expression exhibited by high-grade PCa is associated with poor patient outcome, we used a tissue microarray (TMA) containing 32 cases with multiple disease progression (e.g., Gleason score 6 to 10, T2 or T3). Subsequent to semiquantitative IHC analysis of these clinical samples, the Kaplan-Meier survival curves in Figure 8A indicated that MAOA-low patients had significantly enhanced survival times when compared with MAOA-high patients (log-rank p=0.0286). We further

evaluated the prognostic value of *MAOA* in multiple public clinical DNA microarray data sets using Oncomine 4.4. Considering that PCa is a biologically and clinically heterogeneous disease, we investigated whether high MAOA expression was related to multiple clinical indices in a subset of cases using Cancer Outlier Profile Analysis (COPA), a methodology that has been validated for uncovering candidate oncogenes, such as *ERG* (40, 41). COPA identified *MAOA* as significantly overexpressed in a subset of tumor samples in 15 out of 27 available data sets (gene rank, top 20%; fold change, >2; $p<1 \times 10^{-4}$). Using the same statistical filters, *MAOA* displayed a COPA score comparable to or higher than that of *ERG* in several data sets (Supplemental Table 1).

The Gleason grading system for PCa is a key parameter for clinically assessing prognosis and choice of therapy, and cancers with a higher Gleason score are more aggressive along with a worse prognosis (13). Analysis of 3 data sets (Taylor 3, Glinsky and Bittner) indicated that high-level expression of MAOA was strongly associated with advanced Gleason score (8 to 10) (Figure 8B). We also analyzed MAOA expression profiling in primary and metastatic (lymph node, bone and soft tissues) tumors from 3 data sets (Taylor 3, Holzbeierlein and Varambally). As shown in Figure 8C, MAOA expression was increased when cancer cells formed metastatic lesions after dissemination from the primary site. Invasion of the muscular wall of the seminal vesicles by PCa is considered as a marker for poor prognosis, metastatic disease and quick biochemical recurrence (42). Examining 2 independent data sets (Glinsky and Wallace), we found that PCa patients with seminal vesicle invasion demonstrated higher MAOA expression than patients with intact seminal vesicles (Figure 8D). Additionally, analysis of 2 data sets (Taylor 3 and Glinsky) revealed increased MAOA expression in PCa patients who had biochemical recurrence at 5 years (Figure 8E). Overall, these clinical data support the experimentally described functional roles for MAOA in PCa and further indicate its prognostic value for distinguishing aggressive from indolent PCa.

In summary, our data suggest that the increased intrinsic MAOA in high Gleason grade PCa activates mesenchymal transition and consequent invasive behavior by a mechanism that involves its ability to stabilize HIF1α via ROS production and activate the VEGF-A/NRP1-mediated signaling network, which drives EMT by activating Akt/FoxO1 signaling and enhancing nuclear Twist1 expression (Figure 9). Our data further show the key features of this enhanced cell signaling network in prostate tumor xenograft specimens and in clinical high Gleason grade PCa, supporting the essential roles of MAOA in prostate tumorigenesis and cancer progression.

Discussion

Our study demonstrates for the first time that MAOA plays a pivotal role in repressing the epithelial phenotype and promoting mesenchymal transition to increase the migratory, invasive and metastatic potential of PCa through the regulation of hypoxia and ROS production. MAOA was shown to stabilize HIF1α, activate the VEGF-A/NRP1 system, and induce the expression of Twist1, an EMT master transcription factor commonly associated with EMT promotion. These signaling components downstream from MAOA were shown to be clinically relevant as revealed by the differential expressions of these genes in PCa specimens of different Gleason grades. The clinical relevance of EMT has been shown during tumor progression, and certain typical characteristics including poor differentiation correlated with aggressive and invasive behavior in high Gleason grade PCa can result from EMT and EMT-like processes (43). We observed both increased MAOA expression and EMT in the same specimens of high-grade PCa, which, in line with other data showing that MAOA can drive EMT, provides a molecular basis for the acquisition of a more aggressive phenotype in high Gleason grade PCa. Our observation is consistent with previous studies showing that pharmacological inhibition of MAOA in PCa cells kept basal prostatic epithelial cells from differentiating into matured glandular structures by reorganizing cell structures and decreasing the expressions of basal cytokeratins (9). In addition, a recent clinical survey assessing EMT marker levels in clinical samples with organ-confined PCa revealed that Vimentin and Twist1, among 13 other EMT markers, showed the most promising predictive potential for poor prognosis including biochemical recurrence (44). Our study mechanistically documented the MAOA induction of these two EMT markers along with EMT promotion, and that higher MAOA expression correlated with poor clinical outcomes in PCa patients, again suggesting its potential prognostic value (Figure 8).

Elevated ROS levels in MAOA-overexpressing cells contributed to increased HIF1α stabilization and activity (Figure 3). Significantly, knockdown of MAOA in both cancer cells and tumor xenograft, resulting in reduced ROS levels, decreased HIF1α expression and exerted less hypoxic effect (Supplemental Figure 2, Figures 3 and 7). Several groups have reported the capability of both endogenous and added ROS to either transcriptionally (45) or post-translationally (18) regulate HIF1α activity. We demonstrate that MAOA-produced ROS modulated HIF1α activity by depressing PHD activity, which was further validated by the evidence that the HIF1α transcription level was not directly affected by MAOA (Figures 2 and 3). MAOA, located in the outer membrane of mitochondria, produces hydrogen peroxide as a by-product via its enzymatic reactions, which can be further converted into other species of ROS. In this study, we were able to pinpoint both the intracellular hydrogen peroxide released specifically from intact mitochondria as well as the extracellular general ROS regulated by MAOA in PCa cells (Figure 6 and Supplemental Figure 2). The secreted ROS in the extracellular environment may largely serve as paracrine stimuli to further enhance HIF1α activity via decreased PHD in a heterogeneous tumor cell population. Subsequently, increased HIF1α expression has been found to contribute to increased mitochondrial activity including specific ROS formation during hypoxia (46-48), hence the potential programming of “vicious cycle” or forward feedback loop among MAOA, ROS and HIF1α may further drive increased tumorigenesis.

The ability of MAOA to control VEGF-A/NRP1 signaling by regulating both their expressions establishes a connection between this system and downstream signaling pathways. Since the seminal observations that NRP1 can function as a VEGF co-receptor (24), subsequent studies have demonstrated its functional importance in angiogenesis and cancer development (49). MAOA regulates both the ligand and receptor, and such interactions were exacerbated under hypoxic conditions (Figure 4),

which underscores the function of the VEGF-A/NRP1 signaling system and particularly their EMT-enhancing ability. This finding supports the potential roles of MAOA in distinguishing high Gleason grade PCa that widely shows high tumor angiogenesis activity from low-grade PCa. Apart from the interactions with angiogenic factors, NRP1 also cooperates with other growth factor receptors, such as c-Met (50, 51) and TGFβ receptors (52, 53), to mediate relevant pathways that contribute to tumorigenesis, and therefore could serve as a prognostic marker as well as an attractive target for cancer therapy (49). This establishes an additional rationale for targeting MAOA in PCa therapy whereby patients with high Gleason grade PCa may benefit from the blockade of VEGF-A/NRP1-mediated tumor angiogenesis along with other neuropilin-dependent pathways.

One of the salient features of our study is the discovery that MAOA represses *E-cadherin* transcription and promotes EMT in PCa cells by activating the transcription of *Twist1* via Akt/FoxO1 signaling. We found that MAOA regulates Twist1 most robustly and this pathway could be considered to regulate *E-cadherin* together with other well-characterized EMT master transcription factors such as Snail1 and ZEB1 (54, 55). The mechanisms involved are associated with the regulation of FoxO1 activity by Akt signaling, a transcription factor important for cell death and survival. The direct transcriptional regulation of *Twist1* by FoxO1 proposed for the first time here involves a key response element within the *Twist1* promoter, which is highly conserved in the amniote genomes examined. This finding is supported by our mutational analysis of this element in the *Twist1* promoter as well as the observation that FoxO1 can be recruited to this site *in vivo* (Figure 5). Despite being a consequence of the activation of VEGF-A/NRP1 and Akt signaling, the mechanisms we elucidate for the regulation of Twist1 by MAOA are distinct from the regulation exerted by other genes that promote EMT such as ERβ1, which involves the activation of GSK-3β and Snail1 (14). Of note, such complex but precise selection of pathways to be activated reflects the existence and participation

of other specific factors and machineries that may coordinately contribute to regulation, and will be worthwhile for further investigation.

Our study shows that genetic intervention with MAOA expression, which avoids the potential off-target effects of pharmacological inhibitors, significantly impeded PCa progression or even eliminated prostate tumorigenesis in mice using multiple human and murine prostate carcinoma cell lines to establish tumor xenograft models. The mechanisms discussed here suggest that targeting MAOA blocks PCa tumor growth by disrupting or disengaging the convergent signaling network involving EMT, hypoxia and oxidative stress (Figure 9). Additionally, according to the significant growth-inhibitory effects of targeting MAOA in both human (LNCaP, C4-2 and $ARCaP_M$) and murine (MPC3) PCa cell lines (Figure 6), it is likely that this strategy would blunt the growth and metastasis of aggressive androgen-independent PCa (38, 39).

In summary, we have uncovered the underlying molecular mechanisms contributing to MAOA-initiated PCa progression. MAOA was shown to induce EMT, stabilize HIF1α, and mediate hypoxia-elicited elevation of ROS in prostate carcinomas. Elevated MAOA signals also increased the expression of VEGF and its co-receptor NRP1 that together drive EMT by stimulating Akt/FoxO1 signaling and promoting Twist1 expression. The molecular basis of MAOA action could serve as a prognostic biomarker for poor differentiation and increased aggressiveness of PCa. Targeting MAOA and disengaging its downstream signaling network driving EMT, hypoxia and oxidative stress provide a promising mechanistic rationale for therapeutic development.

Methods

Clinical Specimens. Tissue samples of defined Gleason grades were obtained from the Department of Pathology, Xijing Hospital, Fourth Military Medical University. PCa TMA with patient survival data was obtained from Imgenex (San Diego, CA). Specimens were stained with antibodies specific for MAOA (Santa Cruz, Santa Cruz, CA), E-cadherin (Cell Signaling, Danvers, MA), Vimentin (Santa Cruz), HIF1α (Novus, Littleton, CO), VEGF-A (Santa Cruz), FoxO1 (Millipore, Billerica, MA), pFoxO1 (Millipore) and Twist1 (Sigma, St. Louis, MO) as described previously (56). Additional details on the clinical specimens used and methods of analysis are provided in Supplemental Methods.

Cells and Reagents. Human PCa PC-3 and LNCaP cell lines were obtained from American Type Culture Collection (ATCC, Manassas, VA). The human PCa C4-2 and $ARCaP_M$ cell line was established by our laboratory (39, 57), and the murine PCa MPC3 cell line, bearing a double knockout of Pten and Tp53, was kindly provided by Dr. Neil Bhowmick (Cedars-Sinai Medical Center, Los Angeles, CA). For hypoxia experiments, cells were grown in a hypoxic chamber (1% O_2, 5% CO_2). Human *MAOA* expression construct was generated by inserting the human *MAOA* coding region at *EcoR*I/*Bgl*II sites in 3xFLAG-pCMV vector (Sigma) that contains a neomycin-resistant gene. Human *E-cadherin* promoter luciferase reporter construct (pGL2Basic-EcadK1) was kindly provided by Dr. Eric Fearon (University of Michigan, Ann Arbor, MI) and obtained from Addgene. Human constitutively active (AAA) *FoxO1* expression construct was kindly provided by Dr. Kun-Liang Guan (University of California, San Diego, CA) and obtained from Addgene. Human *Twist1* promoter luciferase reporter constructs of various lengths were kindly provided by Dr. Lu-Hai Wang (The Mount Sinai Hospital, New York, NY). The *Renilla* luciferase plasmid was purchased from Promega (Madison, WI). *MAOA*, *NRP1*, *FoxO1* and non-targeting control shRNA lentiviral particles were purchased from Sigma or Santa Cruz. Human recombinant $VEGF_{165}$ protein was purchased from R&D

Systems (Minneapolis, MN). NAC was purchased from Sigma. DMOG and MG-132 were purchased from Millipore.

Biochemical Analyses. Total RNA was isolated using the RNeasy Mini Kit (Qiagen, Valencia, CA) and reverse-transcribed to cDNA by M-MLV reverse transcriptase (Promega). Details on primers and methods used for qPCR are provided in Supplemental Methods. For immunoblots, cells were extracted with RIPA buffer in the presence of a protease and phosphatase inhibitor cocktail (Thermo Scientific, Rockford, IL), and blots were performed as described previously (58, 59) using primary antibodies against MAOA, N-cadherin (BD Biosciences, San Jose, CA), Twist1 (Santa Cruz), β-Actin (Sigma), HIF1α (BD Biosciences), Lamin B1 (Cell Signaling), hydroxyl-HIF1α (Cell Signaling), pAkt (Ser473) (Cell Signaling), total Akt (Cell Signaling), pFoxO1 (Thr24) (Cell Signaling), total FoxO1 (Santa Cruz), NRP1 (Santa Cruz) and GAPDH (Cell Signaling). Nuclear and cytoplasmic extracts used for immunoblots were prepared with a kit (Thermo Scientific). VEGF-A levels in culture media were quantified by ELISA (R&D Systems).

Migration and Invasion Assays. Assays were performed using 6.5 mm transwell inserts (8 μm pore size) coated with either collagen I or growth factor reduced Matrigel (BD Biosciences) for the migration and invasion assays, respectively. After 18-24 hr, the cells that translocated to the lower surface of the filters were fixed in 4% formaldehyde. The fixed membranes were stained using 1% crystal violet. Assays were quantified by counting the number of stained nuclei in five independent fields in each transwell.

Luciferase Assays. PC-3 cells were transfected with the desired *Firefly* luciferase reporter plasmids and the *Renilla* luciferase construct to normalize for transfection efficiency. Relative light units were calculated as the ratio of *Firefly* luciferase to *Renilla* luciferase activity. The protocol used for transfection and measurement of luciferase activity has been described previously (60).

ROS Measurement. Cellular ROS was measured according to published protocols (61). Briefly, cells were washed with PBS and incubated with 5 μM CM-H_2DCFDA (Life Technologies, Carlsbad, CA) for 30 min. Cells were trypsinized, and mean FL1 fluorescence was measured by flow cytometry. Intact cellular or tumor mitochondria were isolated with a kit (Thermo Scientific) or according to published protocols (62), respectively, and the hydrogen peroxide generation rate measured for a period of 30 min using the AmplexRed Hydrogen Peroxide Assay Kit (Life Technologies) by a spectrophotometer.

Analyses of Twist1 Promoter. Serial deletion analysis of *Twist1* promoter was utilized to locate the putative FoxO1-response element. Site-directed mutagenesis was used to mutate the DRE sequence from (CCAAACT) to (CC*GCG*CT). ChIP analysis was used to determine the direct association of endogenous FoxO1 protein with the native *Twist1* promoter in control and MAOA-overexpressing PC-3 cells. Details of these analyses are provided in Supplemental Methods.

Animal Studies. Animal studies were performed according to a protocol approved by the Institutional Animal Care and Use Committee at Cedars-Sinai Medical Center (CSMC). Male 4- to 6-week-old athymic nude mice or immune-intact C57BL/6 mice were purchased from Taconic (Oxnard, CA), housed in the animal research facility at CSMC, and fed a normal chow diet. For xenograft studies, 1 x 10^6 LNCaP, C4-2 or $ARCaP_M$ (shCon and shMAOA) cells were mixed 1:1 with Matrigel (BD Biosciences) and injected subcutaneously into nude mice. 1 x 10^6 MPC3 (shCon and shMaoa) cells were injected subcutaneously into immune-intact C57BL/6 mice. Each mouse was injected on both flanks. Five to seven mice were used for each group. Tumor size was measured every 2-3 days, and tumors were dissected and weighted after 4-8 weeks. Tumors were fixed in 4% formaldehyde and embedded in paraffin. Sections were stained with hematoxylin and eosin (H&E) in accordance with standard procedures (63).

Immunohistochemistry. IHC analysis of tumor xenograft specimens was performed using antibodies against Ki-67 (Dako, Carpinteria, CA), MAOA, E-cadherin, Vimentin, HIF1α (BD Biosceinces) and VEGF-A as described previously (56). Image acquisition was performed using a Nikon camera and software. Magnification was x400 (scale bars ~20 μm).

MAOA Enzymatic Activity Assay. MAOA enzymatic activity was determined in control and MAOA-KD cells and tumors as described previously (64). Briefly, one hundred micrograms of total protein were incubated with 1 mM [^{14}C]5-HT in the assay buffer at 37^{o}C for 20 min, and the reaction was terminated by the addition of ice-cold 6 N HCl. The reaction products were extracted with benzene/ethyl acetate (1:1) and centrifuged at 4^{o}C for 7 min. The organic phase containing the reaction products was extracted and radioactivity was determined by liquid scintillation spectroscopy.

Statistical Analysis. Data were presented as the mean ± SD as indicated in figure legends. Comparisons between Kaplan-Meier curves were performed using the log-rank test. All other comparisons were analyzed by unpaired Student's t test. A *p* value less than 0.05 is considered as statistically significant.

Supplemental Information

Supplemental Information includes five Supplemental Figures, one Supplemental Table, Supplemental Methods and Supplemental References.

Acknowledgements

This work was supported by NIH Grants 5P01CA098912 (L.W-K.C.) and 5R01MH039085 (J.C.S.), and a DOD Idea Development Award (H.E.Z. and J.C.S.). We thank Dr. Lei Zhang (Fourth Military Medical University, Xi'an, Shaanxi, P.R. China) for providing clinical specimens.

References

1. Siegel, R., Naishadham, D., and Jemal, A. 2013. Cancer statistics, 2013. *CA: a cancer journal for clinicians* 63:11-30.
2. Partin, A.W., Kattan, M.W., Subong, E.N., Walsh, P.C., Wojno, K.J., Oesterling, J.E., Scardino, P.T., and Pearson, J.D. 1997. Combination of prostate-specific antigen, clinical stage, and Gleason score to predict pathological stage of localized prostate cancer. A multi-institutional update. *JAMA : the journal of the American Medical Association* 277:1445-1451.
3. Shih, J.C., Chen, K., and Ridd, M.J. 1999. Monoamine oxidase: from genes to behavior. *Annu Rev Neurosci* 22:197-217.
4. Shih, J.C., Wu, J.B., and Chen, K. 2011. Transcriptional regulation and multiple functions of MAO genes. *Journal of neural transmission* 118:979-986.
5. Bortolato, M., Chen, K., and Shih, J.C. 2008. Monoamine oxidase inactivation: from pathophysiology to therapeutics. *Adv Drug Deliv Rev* 60:1527-1533.
6. Trachootham, D., Alexandre, J., and Huang, P. 2009. Targeting cancer cells by ROS-mediated mechanisms: a radical therapeutic approach? *Nature reviews. Drug discovery* 8:579-591.
7. True, L., Coleman, I., Hawley, S., Huang, C.Y., Gifford, D., Coleman, R., Beer, T.M., Gelmann, E., Datta, M., Mostaghel, E., et al. 2006. A molecular correlate to the Gleason grading system for prostate adenocarcinoma. *Proceedings of the National Academy of Sciences of the United States of America* 103:10991-10996.
8. Peehl, D.M., Coram, M., Khine, H., Reese, S., Nolley, R., and Zhao, H. 2008. The significance of monoamine oxidase-A expression in high grade prostate cancer. *The Journal of urology* 180:2206-2211.

9. Zhao, H., Nolley, R., Chen, Z., Reese, S.W., and Peehl, D.M. 2008. Inhibition of monoamine oxidase A promotes secretory differentiation in basal prostatic epithelial cells. *Differentiation; research in biological diversity* 76:820-830.

10. Nauseef, J.T., and Henry, M.D. 2011. Epithelial-to-mesenchymal transition in prostate cancer: paradigm or puzzle? *Nature reviews. Urology* 8:428-439.

11. Stewart, G.D., Ross, J.A., McLaren, D.B., Parker, C.C., Habib, F.K., and Riddick, A.C. 2010. The relevance of a hypoxic tumour microenvironment in prostate cancer. *BJU international* 105:8-13.

12. Gupta-Elera, G., Garrett, A.R., Robison, R.A., and O'Neill, K.L. 2012. The role of oxidative stress in prostate cancer. *European journal of cancer prevention : the official journal of the European Cancer Prevention Organisation* 21:155-162.

13. Gleason, D.F., and Mellinger, G.T. 1974. Prediction of prognosis for prostatic adenocarcinoma by combined histological grading and clinical staging. *The Journal of urology* 111:58-64.

14. Mak, P., Leav, I., Pursell, B., Bae, D., Yang, X., Taglienti, C.A., Gouvin, L.M., Sharma, V.M., and Mercurio, A.M. 2010. ERbeta impedes prostate cancer EMT by destabilizing HIF-1alpha and inhibiting VEGF-mediated snail nuclear localization: implications for Gleason grading. *Cancer cell* 17:319-332.

15. Lu, X., and Kang, Y. 2010. Hypoxia and hypoxia-inducible factors: master regulators of metastasis. *Clinical cancer research : an official journal of the American Association for Cancer Research* 16:5928-5935.

16. Kaelin, W.G., Jr., and Ratcliffe, P.J. 2008. Oxygen sensing by metazoans: the central role of the HIF hydroxylase pathway. *Molecular cell* 30:393-402.

17. Gerald, D., Berra, E., Frapart, Y.M., Chan, D.A., Giaccia, A.J., Mansuy, D., Pouyssegur, J., Yaniv, M., and Mechta-Grigoriou, F. 2004. JunD reduces tumor angiogenesis by protecting cells from oxidative stress. *Cell* 118:781-794.

18. Finley, L.W., Carracedo, A., Lee, J., Souza, A., Egia, A., Zhang, J., Teruya-Feldstein, J., Moreira, P.I., Cardoso, S.M., Clish, C.B., et al. 2011. SIRT3 opposes reprogramming of cancer cell metabolism through HIF1alpha destabilization. *Cancer cell* 19:416-428.

19. Chandel, N.S., Maltepe, E., Goldwasser, E., Mathieu, C.E., Simon, M.C., and Schumacker, P.T. 1998. Mitochondrial reactive oxygen species trigger hypoxia-induced transcription. *Proceedings of the National Academy of Sciences of the United States of America* 95:11715-11720.

20. Hamanaka, R.B., and Chandel, N.S. 2009. Mitochondrial reactive oxygen species regulate hypoxic signaling. *Current opinion in cell biology* 21:894-899.

21. Antonarakis, E.S., and Carducci, M.A. 2012. Targeting angiogenesis for the treatment of prostate cancer. *Expert opinion on therapeutic targets* 16:365-376.

22. Bartholomeusz, C., and Gonzalez-Angulo, A.M. 2012. Targeting the PI3K signaling pathway in cancer therapy. *Expert opinion on therapeutic targets* 16:121-130.

23. Gross, D.N., van den Heuvel, A.P., and Birnbaum, M.J. 2008. The role of FoxO in the regulation of metabolism. *Oncogene* 27:2320-2336.

24. Soker, S., Takashima, S., Miao, H.Q., Neufeld, G., and Klagsbrun, M. 1998. Neuropilin-1 is expressed by endothelial and tumor cells as an isoform-specific receptor for vascular endothelial growth factor. *Cell* 92:735-745.

25. Bachelder, R.E., Crago, A., Chung, J., Wendt, M.A., Shaw, L.M., Robinson, G., and Mercurio, A.M. 2001. Vascular endothelial growth factor is an autocrine survival factor for neuropilin-expressing breast carcinoma cells. *Cancer research* 61:5736-5740.

26. Yang, J., Mani, S.A., Donaher, J.L., Ramaswamy, S., Itzykson, R.A., Come, C., Savagner, P., Gitelman, I., Richardson, A., and Weinberg, R.A. 2004. Twist, a

master regulator of morphogenesis, plays an essential role in tumor metastasis. *Cell* 117:927-939.

27. Casas, E., Kim, J., Bendesky, A., Ohno-Machado, L., Wolfe, C.J., and Yang, J. 2011. Snail2 is an essential mediator of Twist1-induced epithelial mesenchymal transition and metastasis. *Cancer research* 71:245-254.

28. Vichalkovski, A., Gresko, E., Hess, D., Restuccia, D.F., and Hemmings, B.A. 2010. PKB/AKT phosphorylation of the transcription factor Twist-1 at Ser42 inhibits p53 activity in response to DNA damage. *Oncogene* 29:3554-3565.

29. Xue, G., Restuccia, D.F., Lan, Q., Hynx, D., Dirnhofer, S., Hess, D., Ruegg, C., and Hemmings, B.A. 2012. Akt/PKB-mediated phosphorylation of Twist1 promotes tumor metastasis via mediating cross-talk between PI3K/Akt and TGF-beta signaling axes. *Cancer discovery* 2:248-259.

30. Zhang, Y., Gan, B., Liu, D., and Paik, J.H. 2011. FoxO family members in cancer. *Cancer biology & therapy* 12:253-259.

31. Myatt, S.S., and Lam, E.W. 2007. The emerging roles of forkhead box (Fox) proteins in cancer. *Nature reviews. Cancer* 7:847-859.

32. Shiota, M., Song, Y., Yokomizo, A., Kiyoshima, K., Tada, Y., Uchino, H., Uchiumi, T., Inokuchi, J., Oda, Y., Kuroiwa, K., et al. 2010. Foxo3a suppression of urothelial cancer invasiveness through Twist1, Y-box-binding protein 1, and E-cadherin regulation. *Clinical cancer research : an official journal of the American Association for Cancer Research* 16:5654-5663.

33. Tang, E.D., Nunez, G., Barr, F.G., and Guan, K.L. 1999. Negative regulation of the forkhead transcription factor FKHR by Akt. *The Journal of biological chemistry* 274:16741-16746.

34. Cheng, G.Z., Zhang, W.Z., Sun, M., Wang, Q., Coppola, D., Mansour, M., Xu, L.M., Costanzo, C., Cheng, J.Q., and Wang, L.H. 2008. Twist is transcriptionally

induced by activation of STAT3 and mediates STAT3 oncogenic function. *The Journal of biological chemistry* 283:14665-14673.

35. Glauser, D.A., and Schlegel, W. 2007. The emerging role of FOXO transcription factors in pancreatic beta cells. *The Journal of endocrinology* 193:195-207.

36. Allen, D.L., and Unterman, T.G. 2007. Regulation of myostatin expression and myoblast differentiation by FoxO and SMAD transcription factors. *American journal of physiology. Cell physiology* 292:C188-199.

37. Fan, W., Morinaga, H., Kim, J.J., Bae, E., Spann, N.J., Heinz, S., Glass, C.K., and Olefsky, J.M. 2010. FoxO1 regulates Tlr4 inflammatory pathway signalling in macrophages. *The EMBO journal* 29:4223-4236.

38. Wu, H.C., Hsieh, J.T., Gleave, M.E., Brown, N.M., Pathak, S., and Chung, L.W. 1994. Derivation of androgen-independent human LNCaP prostatic cancer cell sublines: role of bone stromal cells. *International journal of cancer. Journal international du cancer* 57:406-412.

39. Zhau, H.Y., Chang, S.M., Chen, B.Q., Wang, Y., Zhang, H., Kao, C., Sang, Q.A., Pathak, S.J., and Chung, L.W. 1996. Androgen-repressed phenotype in human prostate cancer. *Proceedings of the National Academy of Sciences of the United States of America* 93:15152-15157.

40. Tomlins, S.A., Rhodes, D.R., Perner, S., Dhanasekaran, S.M., Mehra, R., Sun, X.W., Varambally, S., Cao, X., Tchinda, J., Kuefer, R., et al. 2005. Recurrent fusion of TMPRSS2 and ETS transcription factor genes in prostate cancer. *Science* 310:644-648.

41. Yoshioka, T., Otero, J., Chen, Y., Kim, Y.M., Koutcher, J.A., Satagopan, J., Reuter, V., Carver, B., de Stanchina, E., Enomoto, K., et al. 2013. beta4 Integrin signaling induces expansion of prostate tumor progenitors. *The Journal of clinical investigation* 123:682-699.

42. Potter, S.R., Epstein, J.I., and Partin, A.W. 2000. Seminal vesicle invasion by prostate cancer: prognostic significance and therapeutic implications. *Reviews in urology* 2:190-195.

43. Savagner, P. 2010. The epithelial-mesenchymal transition (EMT) phenomenon. *Annals of oncology : official journal of the European Society for Medical Oncology / ESMO* 21 Suppl 7:vii89-92.

44. Behnsawy, H.M., Miyake, H., Harada, K., and Fujisawa, M. 2013. Expression patterns of epithelial-mesenchymal transition markers in localized prostate cancer: significance in clinicopathological outcomes following radical prostatectomy. *BJU international* 111:30-37.

45. Bonello, S., Zahringer, C., BelAiba, R.S., Djordjevic, T., Hess, J., Michiels, C., Kietzmann, T., and Gorlach, A. 2007. Reactive oxygen species activate the HIF-1alpha promoter via a functional NFkappaB site. *Arteriosclerosis, thrombosis, and vascular biology* 27:755-761.

46. Guzy, R.D., Hoyos, B., Robin, E., Chen, H., Liu, L., Mansfield, K.D., Simon, M.C., Hammerling, U., and Schumacker, P.T. 2005. Mitochondrial complex III is required for hypoxia-induced ROS production and cellular oxygen sensing. *Cell metabolism* 1:401-408.

47. Chandel, N.S., McClintock, D.S., Feliciano, C.E., Wood, T.M., Melendez, J.A., Rodriguez, A.M., and Schumacker, P.T. 2000. Reactive oxygen species generated at mitochondrial complex III stabilize hypoxia-inducible factor-1alpha during hypoxia: a mechanism of O2 sensing. *The Journal of biological chemistry* 275:25130-25138.

48. Schroedl, C., McClintock, D.S., Budinger, G.R., and Chandel, N.S. 2002. Hypoxic but not anoxic stabilization of HIF-1alpha requires mitochondrial reactive oxygen

species. *American journal of physiology. Lung cellular and molecular physiology* 283:L922-931.

49. Guttmann-Raviv, N., Kessler, O., Shraga-Heled, N., Lange, T., Herzog, Y., and Neufeld, G. 2006. The neuropilins and their role in tumorigenesis and tumor progression. *Cancer letters* 231:1-11.

50. Matsushita, A., Gotze, T., and Korc, M. 2007. Hepatocyte growth factor-mediated cell invasion in pancreatic cancer cells is dependent on neuropilin-1. *Cancer research* 67:10309-10316.

51. Hu, B., Guo, P., Bar-Joseph, I., Imanishi, Y., Jarzynka, M.J., Bogler, O., Mikkelsen, T., Hirose, T., Nishikawa, R., and Cheng, S.Y. 2007. Neuropilin-1 promotes human glioma progression through potentiating the activity of the HGF/SF autocrine pathway. *Oncogene* 26:5577-5586.

52. Glinka, Y., and Prud'homme, G.J. 2008. Neuropilin-1 is a receptor for transforming growth factor beta-1, activates its latent form, and promotes regulatory T cell activity. *Journal of leukocyte biology* 84:302-310.

53. Cao, S., Yaqoob, U., Das, A., Shergill, U., Jagavelu, K., Huebert, R.C., Routray, C., Abdelmoneim, S., Vasdev, M., Leof, E., et al. 2010. Neuropilin-1 promotes cirrhosis of the rodent and human liver by enhancing PDGF/TGF-beta signaling in hepatic stellate cells. *The Journal of clinical investigation* 120:2379-2394.

54. Batlle, E., Sancho, E., Franci, C., Dominguez, D., Monfar, M., Baulida, J., and Garcia De Herreros, A. 2000. The transcription factor snail is a repressor of E-cadherin gene expression in epithelial tumour cells. *Nature cell biology* 2:84-89.

55. Comijn, J., Berx, G., Vermassen, P., Verschueren, K., van Grunsven, L., Bruyneel, E., Mareel, M., Huylebroeck, D., and van Roy, F. 2001. The two-handed E box binding zinc finger protein SIP1 downregulates E-cadherin and induces invasion. *Molecular cell* 7:1267-1278.

56. Hu, P., Chu, G.C., Zhu, G., Yang, H., Luthringer, D., Prins, G., Habib, F., Wang, Y., Wang, R., Chung, L.W., et al. 2011. Multiplexed quantum dot labeling of activated c-Met signaling in castration-resistant human prostate cancer. *PloS one* 6:e28670.

57. Thalmann, G.N., Anezinis, P.E., Chang, S.M., Zhau, H.E., Kim, E.E., Hopwood, V.L., Pathak, S., von Eschenbach, A.C., and Chung, L.W. 1994. Androgen-independent cancer progression and bone metastasis in the LNCaP model of human prostate cancer. *Cancer research* 54:2577-2581.

58. Zeng, N., Li, Y., He, L., Xu, X., Galicia, V., Deng, C., and Stiles, B.L. 2011. Adaptive basal phosphorylation of eIF2alpha is responsible for resistance to cellular stress-induced cell death in Pten-null hepatocytes. *Molecular cancer research : MCR* 9:1708-1717.

59. Chen, K., Ou, X.M., Wu, J.B., and Shih, J.C. 2011. Transcription factor E2F-associated phosphoprotein (EAPP), RAM2/CDCA7L/JPO2 (R1), and simian virus 40 promoter factor 1 (Sp1) cooperatively regulate glucocorticoid activation of monoamine oxidase B. *Molecular pharmacology* 79:308-317.

60. Wu, J.B., and Shih, J.C. 2011. Valproic acid induces monoamine oxidase A via Akt/forkhead box O1 activation. *Molecular pharmacology* 80:714-723.

61. Eruslanov, E., and Kusmartsev, S. 2010. Identification of ROS using oxidized DCFDA and flow-cytometry. *Methods in molecular biology* 594:57-72.

62. Graham, J.M. 2001. Isolation of mitochondria from tissues and cells by differential centrifugation. *Current protocols in cell biology / editorial board, Juan S. Bonifacino ... [et al.]* Chapter 3:Unit 3 3.

63. Fischer, A.H., Jacobson, K.A., Rose, J., and Zeller, R. 2008. Hematoxylin and eosin staining of tissue and cell sections. *CSH protocols* 2008:pdb prot4986.

64. Wu, J.B., Chen, K., Li, Y., Lau, Y.F., and Shih, J.C. 2009. Regulation of monoamine oxidase A by the SRY gene on the Y chromosome. *FASEB journal : official publication of the Federation of American Societies for Experimental Biology* 23:4029-4038.

Figure Legends

Figure 1. MAOA and EMT in PCa. (**A**) Clinical specimens of normal prostatic epithelium and Gleason grade 3 and 5 PCa were stained for E-cadherin, Vimentin and MAOA. Representative images from three separate specimens are shown. Original magnification, x400; scale bars represent 20 μm. (**B**) PC-3 cells stably overexpressing an empty vector or MAOA were photographed and extracts were analyzed for the expression of MAOA and EMT markers. Original magnification, x40; scale bars represent 200 μm. (**C**) PC-3 cells stably overexpressing an empty vector or MAOA were transfected with an *E-cadherin* promoter reporter construct (Vector+ and MAOA+) or pGL2 Basic vector (Vector and MAOA) as a control, and assayed for luciferase activity. The data represent the mean ± SD of *Firefly* luciferase activity normalized to *Renilla* luciferase activity from three separate experiments. The *E-cadherin* promoter activity in vector-expressing PC-3 cells was set as 100%. **, $p<0.01$. (**D**) Immunoblots of LNCaP cells that express a *MAOA*-targeting shRNA (shMAOA) or a scrambled shRNA (shCon) for MAOA and E-cadherin. Expression of *MAOA*, *Vimentin* and *N-cadherin* mRNA in these cells was also measured by qRT-PCR. **, $p<0.01$. (**E, F**) PC-3 (Vector and MAOA-overexpression) and LNCaP (shCon and shMAOA) cells were assessed for their ability to either migrate (**E**) or invade (**F**). The data represent the mean ± SD of three separate experiments. The migration or invasion of respective control cells was set as 100%. **, $p<0.01$.

Figure 2. MAOA regulates HIF1α stability. (**A**) Immunoblots of nuclear extracts from PC-3 cells that stably express an empty vector or MAOA cultured at 21% O_2. (**B, D**) Immunoblots of PC-3 (Vector and MAOA-overexpression) (**B**) or LNCaP (shCon and shMAOA) (**D**) cells cultured at 1% O_2 for the indicated times. (**C, E**) Fold induction of HIF1α target genes in PC-3 (Vector and MAOA-overexpression) (**C**) or LNCaP (shCon

and shMAOA) (**E**) cells after 24 hr of hypoxia were measured by qRT-PCR and shown as normalized to control group normoxia levels. *, $p<0.05$, **, $p<0.01$.

Figure 3. MAOA regulates HIF1α stability through ROS. (**A**) PC-3 cells (Vector and MAOA-overexpression) treated with or without 1 μM MG-132 for 6 hr were immunoblotted with antibodies specific to hydroxylated HIF1α (HIF1α-OH) and total HIF1α. (**B**) Fold induction of HIF1α target genes in PC-3 cells (Vector and MAOA-overexpression) in response to 1 mM DMOG treatment for 24 hr was measured by qRT-PCR, and the ratio of DMOG-treated to untreated gene expression is shown. *, $p<0.05$, **, $p<0.01$. (**C**) The increase in ROS production in PC-3 cells (Vector and MAOA-overexpression) with hypoxia was calculated as the percentage change in ROS in hypoxic cells relative to normoxic controls. **, $p<0.01$. (**D**) Immunoblots of PC-3 cells (Vector and MAOA-overexpression) were incubated with 10 mM NAC and cultured under normoxia and hypoxia. (**E**) Immunoblots of PC-3 cells (Vector and MAOA-overexpression) were cultured at 21% O_2 with 10 mM NAC or 1 mM DMOG as indicated. (**F**) *VEGF-A*, *Glut1* and *Twist1* expression were measured by qRT-PCR in PC-3 cells (Vector and MAOA-overexpression) incubated with 10 mM NAC and cultured under hypoxia. **, $p<0.01$, ns, not significant. (**G**) Growth curves of PC-3 cells (Vector and MAOA-overexpression) cultured in standard media supplemented with or without 10 mM NAC. The data represent the mean ± SD from three separate experiments. *, $p<0.05$, **, $p<0.01$. (H) A schematic diagram showing MAOA stabilization of HIF1α by repressing PHD activity through ROS production.

Figure 4. MAOA promotes VEGF- and its receptor NRP1-mediated activation of Akt/FoxO1 signaling. (**A**) *VEGF-A* mRNA expression was measured by qRT-PCR in PC-3 (Vector and MAOA-overexpression) and LNCaP (shCon and shMAOA) cells. VEGF-A

secretion in culture media from these cells was quantified by ELISA. *, $p<0.05$, **, $p<0.01$. (**B**) PC-3 cells treated with or without recombinant $VEGF_{165}$ (50 ng/ml) were immunoblotted with antibodies specific to pAkt (Ser473), pFoxO1 (Thr24), total Akt and total FoxO1. (**C**) Immunoblots of PC-3 (Vector and MAOA-overexpression) and LNCaP (shCon and shMAOA) cells with antibodies specific to pAkt (Ser473), pFoxO1 (Thr24), total Akt and total FoxO1. (**D**) PC-3 cells (Vector and MAOA-overexpression) that express a *NRP1*-targeting shRNA (shNRP1) or a scrambled shRNA (shCon) were immunoblotted with antibodies specific to NRP1, pAkt (Ser473), pFoxO1 (Thr24), total Akt and total FoxO1. (**E**) Immunoblots of nuclear and cytoplasmic extracts from different groups of PC-3 cells (Vector and MAOA, untreated and VEGF-treated, shCon and shNRP1) for FoxO1. Lamin B1 and GAPDH serve as nuclear and cytoplasmic protein markers, respectively. (**F**) IHC analysis of MAOA, HIF1α, VEGF-A and NRP1 expression in PC-3 (Vector and MAOA-overexpression) tumor xenografts. Representative images from three separate samples are shown. Original magnification, x400; scale bars represent 20 μm. (**G**) PC-3 cells as established in (**D**) were assessed for their ability to either migrate or invade. The data represent the mean ± SD from three separate experiments. The migration or invasion of control cells (Vector + shCon) was set as 100%. *,$p<0.05$, **, $p<0.01$. (**H**) Growth curves of PC-3 cells as established in (**D**). The data represent the mean ± SD from three separate experiments. **, $p<0.01$.

Figure 5. MAOA activates Twist1 by reducing FoxO1 activity. (**A**) *Twist1* mRNA expression was measured by qRT-PCR in PC-3 (Vector and MAOA-overexpression) and LNCaP (shCon and shMAOA) cells. A human *Twist1* promoter reporter construct was transfected into these cells, and the luciferase activity was assayed. *, $p<0.05$, **, $p<0.01$. (**B**) PC-3 cells that stably overexpress an empty vector or a constitutively active *FoxO1* (AAA *FoxO1*) construct, and PC-3 cells that stably express a *FoxO1*-targeting shRNA

(shFoxO1) or a scrambled shRNA (shCon) were immunoblotted with antibody against Twist1. (**C**) *Twist1* mRNA expression was measured by qRT-PCR in PC-3 (Vector and AAA FoxO1-overexpression, shCon and shFoxO1) cells. (**D**) PC-3 cells were transiently transfected with a *Twist1* promoter reporter construct together with an empty vector, an AAA *FoxO1* construct or a mutant AAA *FoxO1* (H215R, deficient in DNA-binding ability) construct, or PC-3 cells (shCon and shFoxO1) were transiently transfected with a *Twist1* promoter reporter construct, and the luciferase activity was assayed. **, $p<0.01$, ns, not significant. (**E**) The canonical binding sequence for FoxO1-mediated transcriptional regulation (upper sequence), a potential FoxO1-binding site in *Twist1* promoter that is 50-56 bp upstream from the first transcription initiation site (middle sequence), and introduced point mutations (italic and in red, lower sequence) used to inactivate the potential FoxO1-binding site (upper box). Alignment of the conserved FoxO1-binding site (bold) in *Twist1* promoter across different species is shown, and the starting number of the sequence indicates the distance from transcription initiation sites (lower box). (**F, G**) PC-3 cells (**F**, Vector and AAA FoxO1, or **G**, Vector and MAOA) cells were transiently transfected with the wild-type (WT) or mutant (Mut) *Twist1* promoter reporter construct, and the luciferase activity was assayed. **, $p<0.01$, ns, not significant. (**H**) Chromatin from PC-3 (Vector and MAOA) cells was immunoprecipitated using FoxO1 or IgG antibody and qRT-PCR was conducted using 1 primer set for the FoxO1-binding region in *Twist1* promoter and 1 control primer set for *Twist1* exon1. The data represent the mean ± SD reflecting the percent of input from three separate experiments. *, $p<0.05$.

Figure 6. MAOA is essential for the growth of prostate tumor xenografts by regulating EMT, hypoxia and ROS. (**A**) LNCaP, C4-2, $ARCaP_M$ or MPC3 cells that stably express a *MAOA*-targeting shRNA (shMAOA) or a scrambled shRNA (shCon) were subcutaneously injected into male nude mice (N=5-7 for each group) for the growth of

tumor xenografts. Tumor growth was determined by measuring tumor volume, tumor weight and the frequency of tumor formation. *, $p<0.05$, **, $p<0.01$. (**B**) H&E and IHC analysis of Ki-67, MAOA, E-cadherin, Vimentin, HIF1α and VEGF-A expression in LNCaP (shCon and shMAOA) tumor xenografts. Representative images from five separate samples are shown. Original magnification, x400; scale bars represent 20 μm. (**C**) Quantification of percent of Ki-67$^+$ tumor cells in LNCaP (shCon and shMAOA) and C4-2 (shCon and shMAOA) tumor xenografts from five distinct images of each tumor sample (N=5 for each group). The data represent mean ± SD. *, $p<0.05$, **, $p<0.01$. (**D**) Determination of MAOA enzymatic activity in LNCaP (shCon and shMAOA) and C4-2 (shCon and shMAOA) tumor xenografts. The data represent mean ± SD from all tumors obtained at mouse sacrifice (N=6-15 for each group). **, $p<0.01$. (**E**) Determination of H_2O_2 generation rate in intact mitochondria isolated from LNCaP (shCon and shMAOA) and C4-2 (shCon and shMAOA) tumor xenografts (N=3) by Amplex Red hydrogen peroxide assay. The data represent mean ± SD. *, $p<0.05$.

Figure 7. The HIF1α/VEGF/FoxO1/Twist1 pathway is manifested in high Gleason grade PCa. (**A**) Thirty specimens of human PCa including 15 Gleason grade 3 tumors and 15 Gleason grade 5 tumors were immunostained for MAOA, HIF1α, VEGF-A, FoxO1, pFoxO1 and Twist1. Original magnification, x400; scale bars represent 20 μm. (**B**) Semiquantitative analysis of IHC staining was performed for all specimens to assess both the percentage of cells stained and the intensity of each staining. This analysis is reported as the Quotient (Q) of these two parameters (mean ± SD). The significance of the difference in Q between Gleason grade 3 and 5 as determined by Student's t test is shown for each bar graph. Images representative of the mean Q for each IHC staining are shown.

Figure 8. Increased MAOA expression is associated with poor prognosis in PCa patients. (**A**) Kaplan-Meier plots of survival of PCa patients stratified by the expression of MAOA from TMA (32 patients in total; MAOA-low, N=16; MAOA-high, N=16). The *p* value was calculated by a log-rank test. (**B-E**) Oncomine analyses of MAOA transcript level in publically available DNA microarray data sets regarding Gleason score (**B**), cancer sample site (**C**), seminal vesicle involvement (**D**), and 5-year recurrence status (**E**). *, $p<0.05$, **, $p<0.01$.

Figure 9. Proposed model for how MAOA regulates prostate tumorigenesis by engaging EMT, hypoxia and ROS. MAOA induces EMT by generating ROS that inhibit PHD activity and stabilizing HIF1α, and stimuli such as hypoxia can exacerbate ROS production by MAOA. MAOA-mediated activation of VEGF-A/NRP1 signaling activates the Akt/FoxO1 pathway, which results in the nuclear export of transcription repressor FoxO1 and promotes nuclear Twist1 expression. Together, increased MAOA expression promotes EMT, hypoxia and ROS production, which in concert drive PCa tumorigenesis and progression.

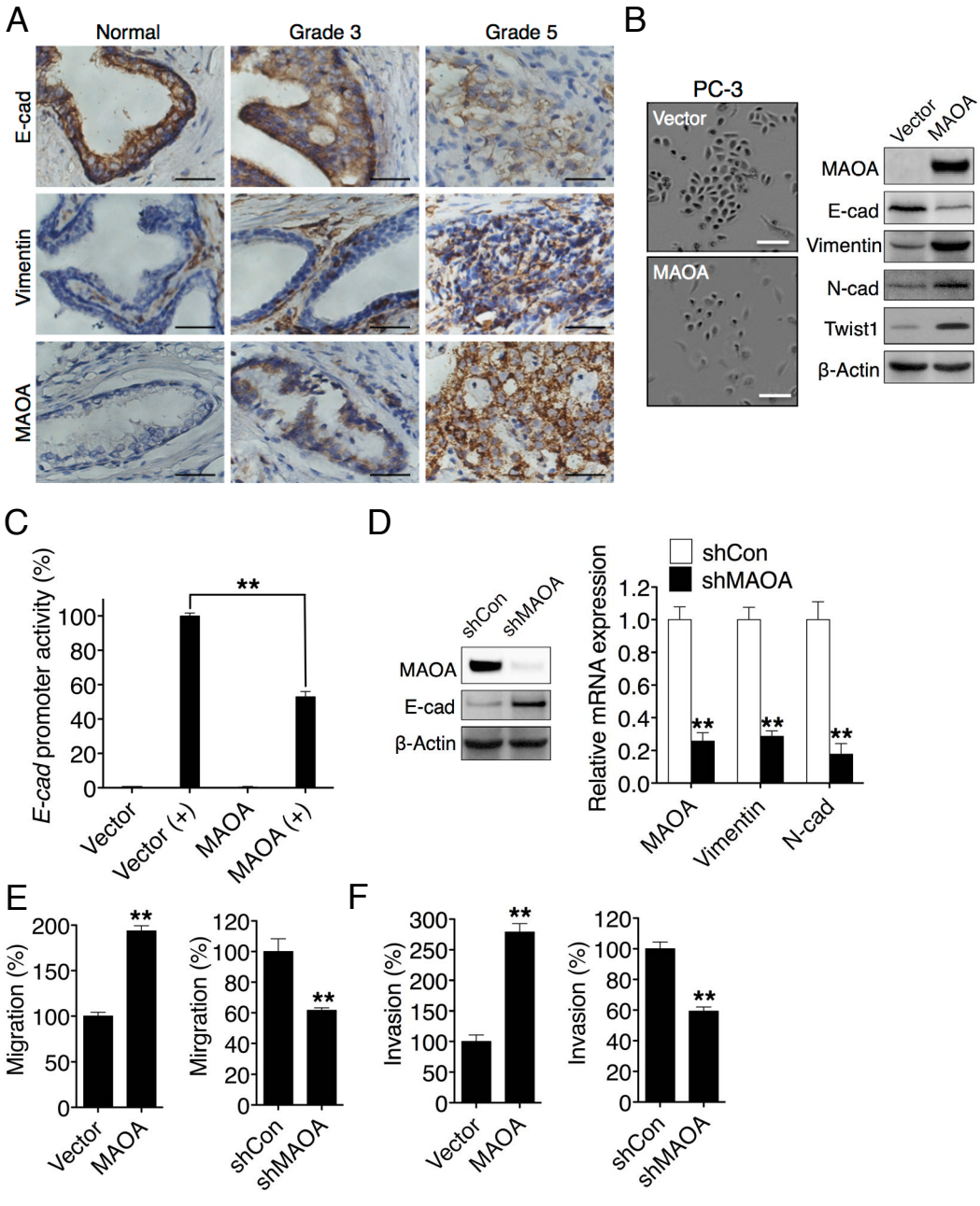
A
Normal
Grade 3
Grade 5
E-cad
Vimentin
MAOA
B
PC-3
Vector
MAOA
Vector
MAOA
E-cad
Vimentin
N-cad
Twist1
β-Actin
C
E-cad promoter activity (%)
**
Vector
Vector (+)
MAOA
MAOA (+)
D
shCon
shMAOA
MAOA
E-cad
β-Actin
shCon
shMAOA
Relative mRNA expression
MAOA
Vimentin
N-cad
E
Migration (%)
Vector
MAOA
Mirgration (%)
shCon
shMAOA
F
Invasion (%)
Vector
MAOA
Invasion (%)
shCon
shMAOA

Wu et al Fig 1

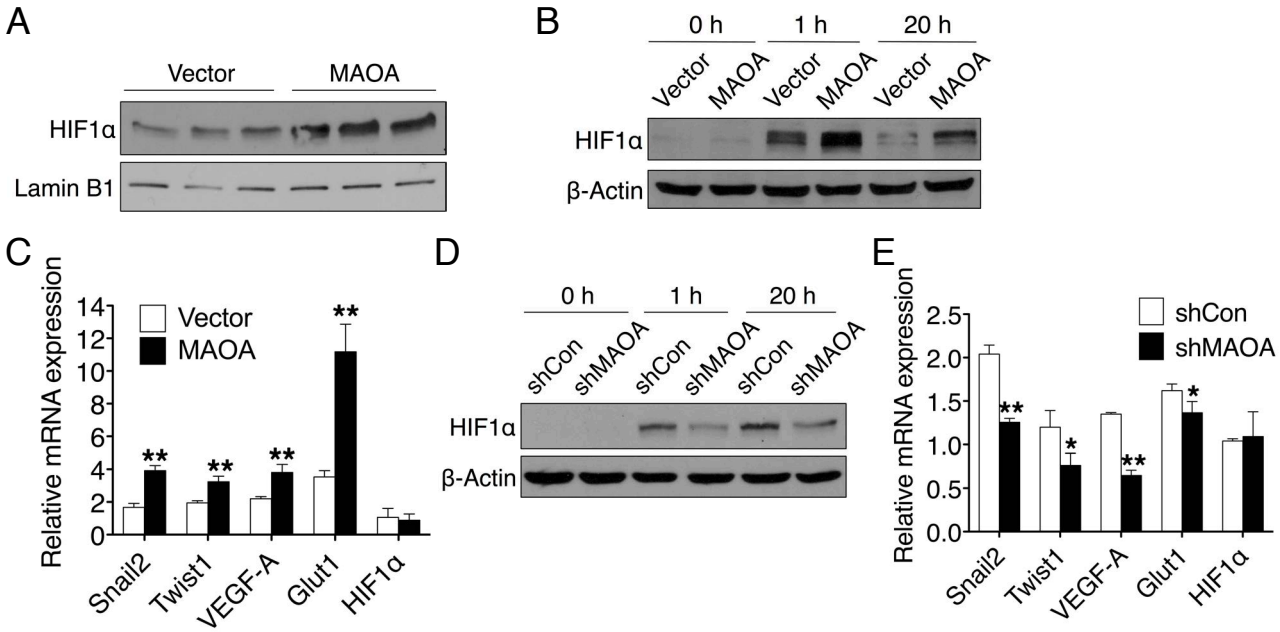
A
Vector
MAOA
HIF1α
Lamin B1
B
0 h
1 h
20 h
Vector
MAOA
Vector
MAOA
Vector
MAOA
HIF1α
β-Actin
C
Relative mRNA expression
Vector
MAOA
Snail2
Twist1
VEGF-A
Glut1
HIF1α
D
0 h
1 h
20 h
shCon
shMAOA
shCon
shMAOA
shCon
shMAOA
HIF1α
β-Actin
E
Relative mRNA expression
shCon
shMAOA
Snail2
Twist1
VEGF-A
Glut1
HIF1α

Wu et al Fig 2

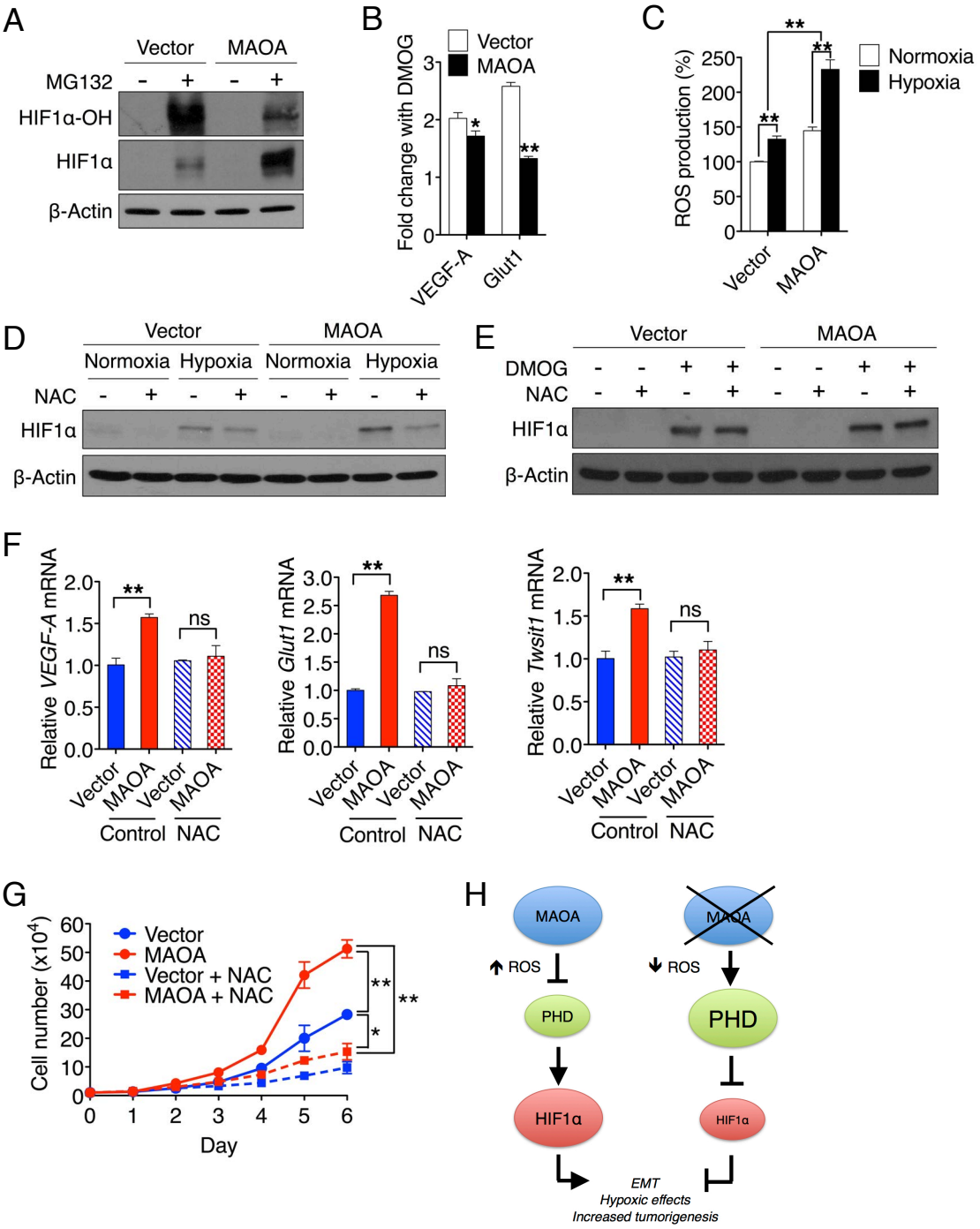
A
Vector
MAOA
MG132
HIF1α-OH
HIF1α
β-Actin
B
Vector
MAOA
Fold change with DMOG
VEGF-A
Glut1
C
Normoxia
Hypoxia
ROS production (%)
Vector
MAOA
D
Vector
MAOA
Normoxia
Hypoxia
NAC
HIF1α
β-Actin
E
DMOG
NAC
HIF1α
β-Actin
F
Relative VEGF-A mRNA
Relative Glut1 mRNA
Relative Twsit1 mRNA
ns
Control
NAC
G
Vector
MAOA
Vector + NAC
MAOA + NAC
Cell number (x10⁴)
Day
H
MAOA
ROS
PHD
HIF1α
EMT
Hypoxic effects
Increased tumorigenesis

Wu et al Fig 3

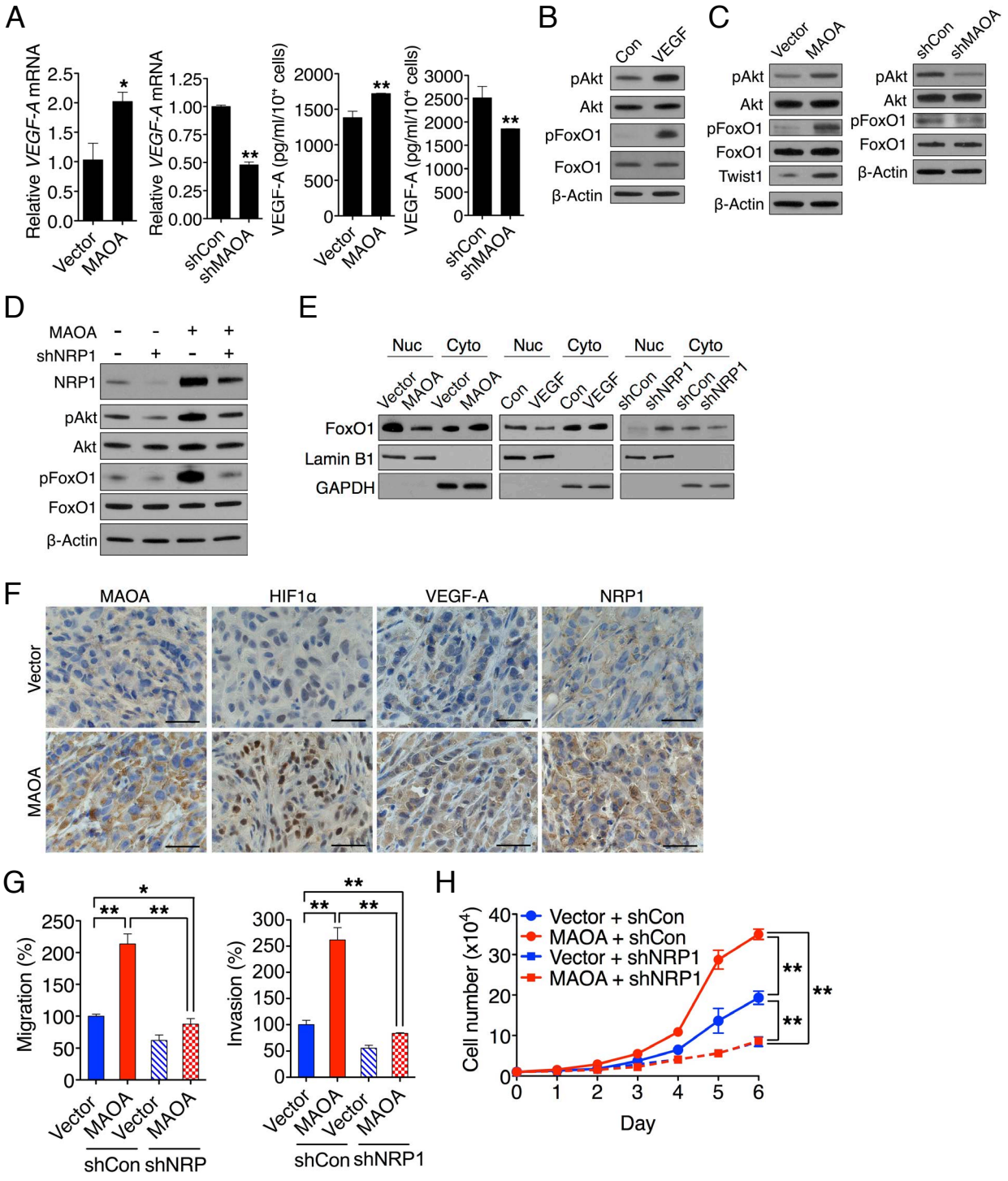
A
Relative VEGF-A mRNA
Vector
MAOA
shCon
shMAOA
VEGF-A (pg/ml/10⁴ cells)
B
Con
VEGF
pAkt
Akt
pFoxO1
FoxO1
β-Actin
C
Vector
MAOA
shCon
shMAOA
Twist1
D
MAOA
shNRP1
NRP1
E
Nuc
Cyto
Lamin B1
GAPDH
F
MAOA
HIF1α
VEGF-A
NRP1
G
Migration (%)
Invasion (%)
shCon shNRP
shCon shNRP1
H
Cell number (x10⁴)
Vector + shCon
MAOA + shCon
Vector + shNRP1
MAOA + shNRP1
Day

Wu et al Fig 4

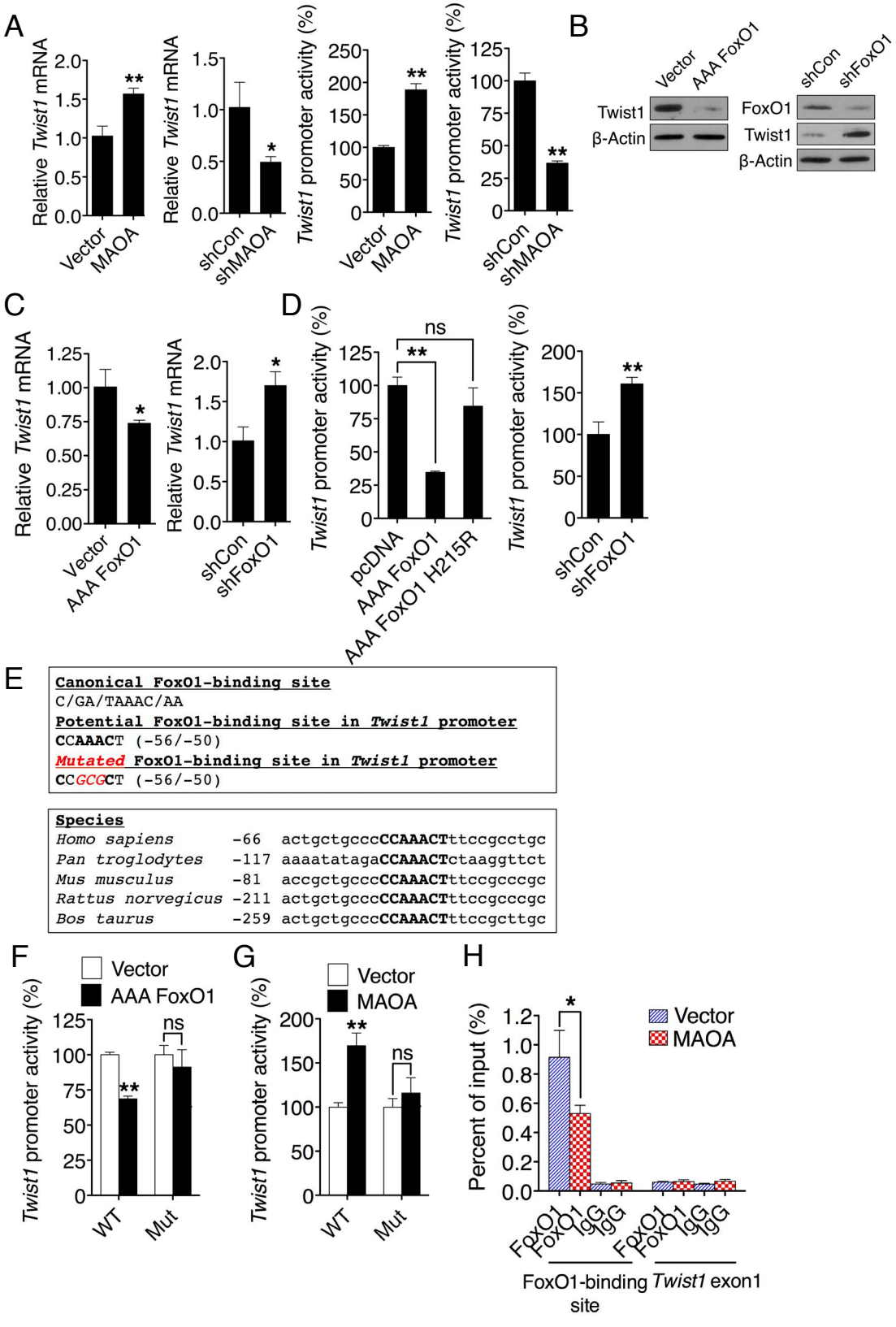
A
Relative Twist1 mRNA
Vector
MAOA
shCon
shMAOA
Twist1 promoter activity (%)
B
Vector
AAA FoxO1
shCon
shFoxO1
Twist1
β-Actin
FoxO1
C
Relative Twist1 mRNA
Vector
AAA FoxO1
shCon
shFoxO1
D
Twist1 promoter activity (%)
ns
pcDNA
AAA FoxO1
AAA FoxO1 H215R
E
Canonical FoxO1-binding site
C/GA/TAAAC/AA
Potential FoxO1-binding site in Twist1 promoter
CCAAACT (-56/-50)
Mutated FoxO1-binding site in Twist1 promoter
CCGCGCT (-56/-50)
Species
Homo sapiens -66 actgctgcccCCAAACTttccgcctgc
Pan troglodytes -117 aaaatatagaCCAAACTctaaggttct
Mus musculus -81 accgctgcccCCAAACTttccgcccgc
Rattus norvegicus -211 actgctgcccCCAAACTttccgcccgc
Bos taurus -259 actgctgcccCCAAACTttccgcttgc
F
Vector
AAA FoxO1
WT
Mut
G
Vector
MAOA
H
Percent of input (%)
Vector
MAOA
FoxO1
IgG
FoxO1-binding Twist1 exon1 site

Wu et al Fig 5

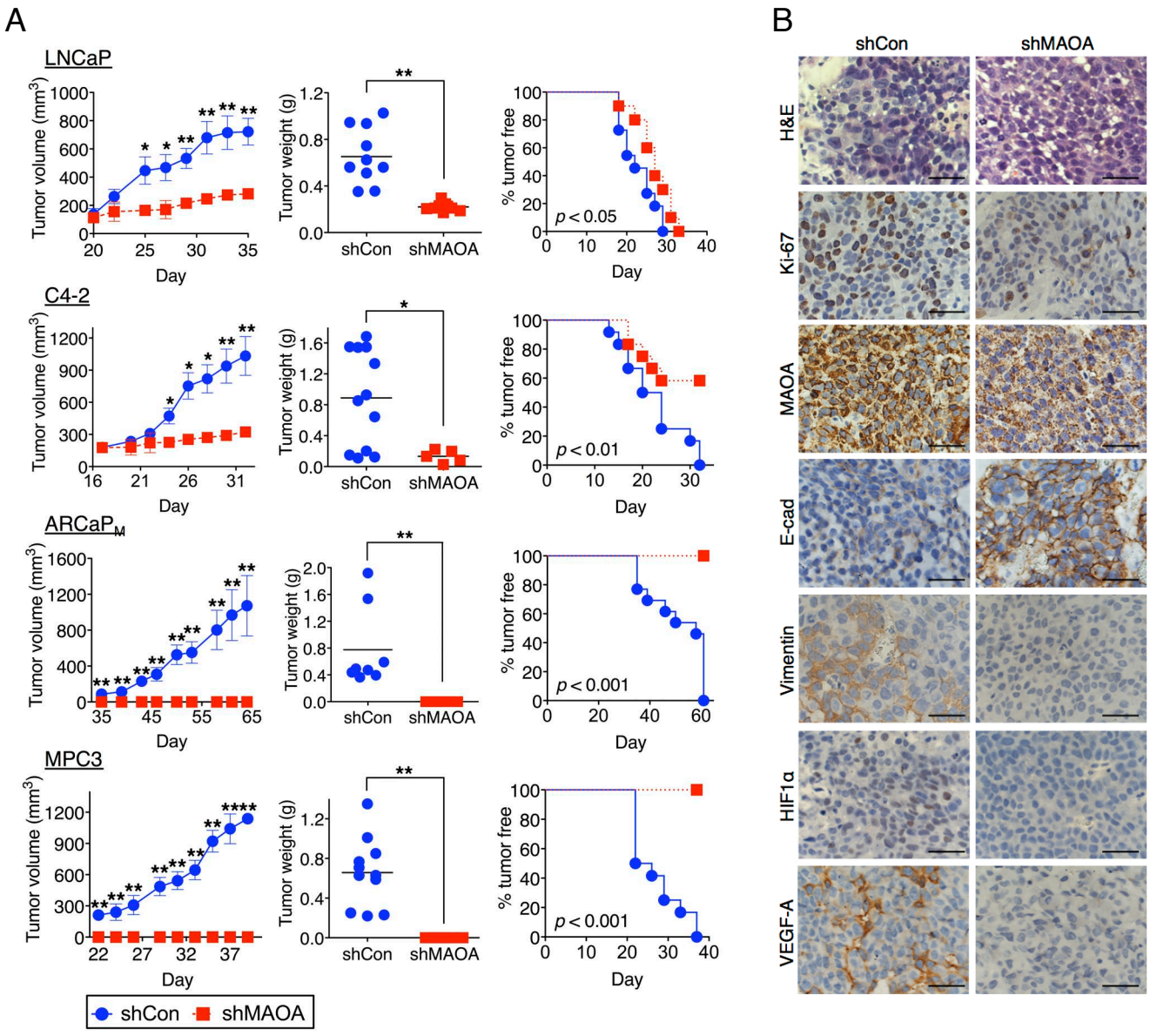
A
LNCaP
C4-2
ARCaP$_M$
MPC3
Tumor volume (mm^3)
Day
Tumor weight (g)
shCon
shMAOA
% tumor free
$p < 0.05$
$p < 0.01$
$p < 0.001$
shCon
shMAOA
B
shCon
shMAOA
H&E
Ki-67
MAOA
E-cad
Vimentin
HIF1α
VEGF-A
C
Ki-67$^+$ cells (%)
shCon
shMAOA
LNCaP
C4-2
D
MAOA catalytic activity (nmol/20 min/mg protein)
shCon
shMAOA
LNCaP
C4-2
E
H_2O_2 generation rate (μM/min/mg mito)
shCon
shMAOA
LNCaP
C4-2

Wu et al Fig 6

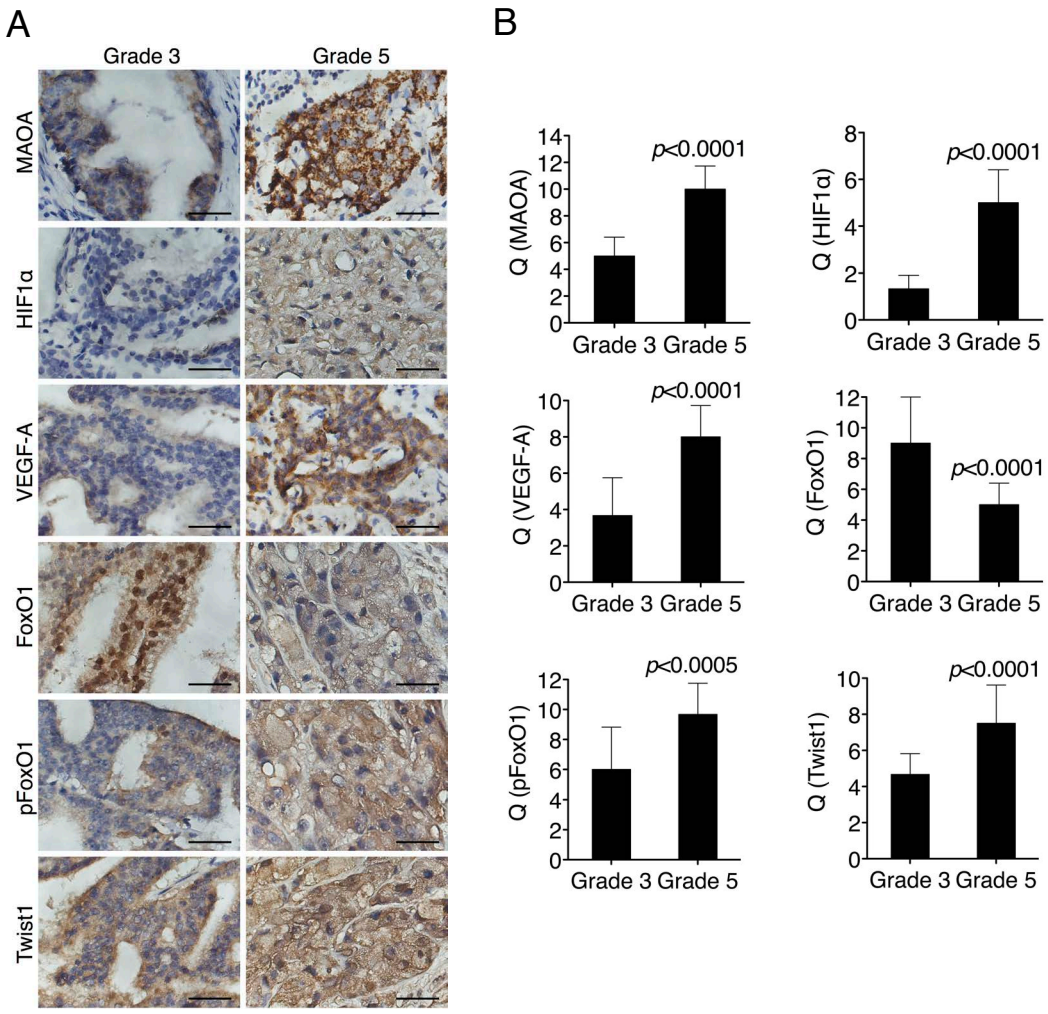
A
Grade 3
Grade 5
MAOA
HIF1α
VEGF-A
FoxO1
pFoxO1
Twist1
B
Q (MAOA)
p<0.0001
Grade 3 Grade 5
Q (HIF1α)
p<0.0001
Grade 3 Grade 5
Q (VEGF-A)
p<0.0001
Grade 3 Grade 5
Q (FoxO1)
p<0.0001
Grade 3 Grade 5
Q (pFoxO1)
p<0.0005
Grade 3 Grade 5
Q (Twist1)
p<0.0001
Grade 3 Grade 5

Wu et al Fig 7

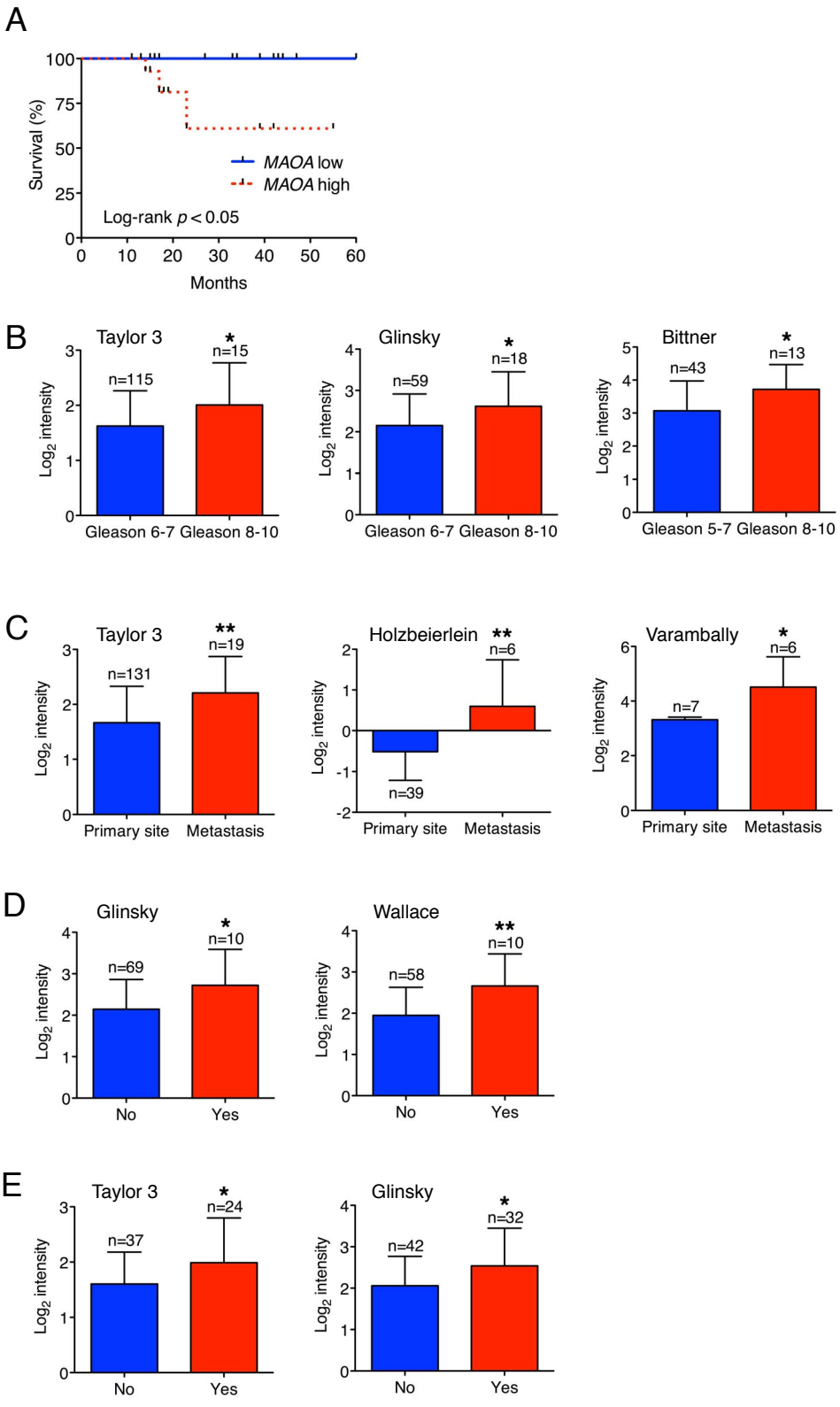
A
Survival (%)
100
75
50
25
0
MAOA low
MAOA high
Log-rank p < 0.05
0 10 20 30 40 50 60
Months
B
Taylor 3
n=115
*
n=15
Log2 intensity
Gleason 6-7 Gleason 8-10
Glinsky
n=59
*
n=18
Gleason 6-7 Gleason 8-10
Bittner
n=43
*
n=13
Gleason 5-7 Gleason 8-10
C
Taylor 3
n=131
**
n=19
Primary site Metastasis
Holzbeierlein
n=39
**
n=6
Primary site Metastasis
Varambally
n=7
*
n=6
Primary site Metastasis
D
Glinsky
n=69
*
n=10
No Yes
Wallace
n=58
**
n=10
No Yes
E
Taylor 3
n=37
*
n=24
No Yes
Glinsky
n=42
*
n=32
No Yes

Wu et al Fig 8

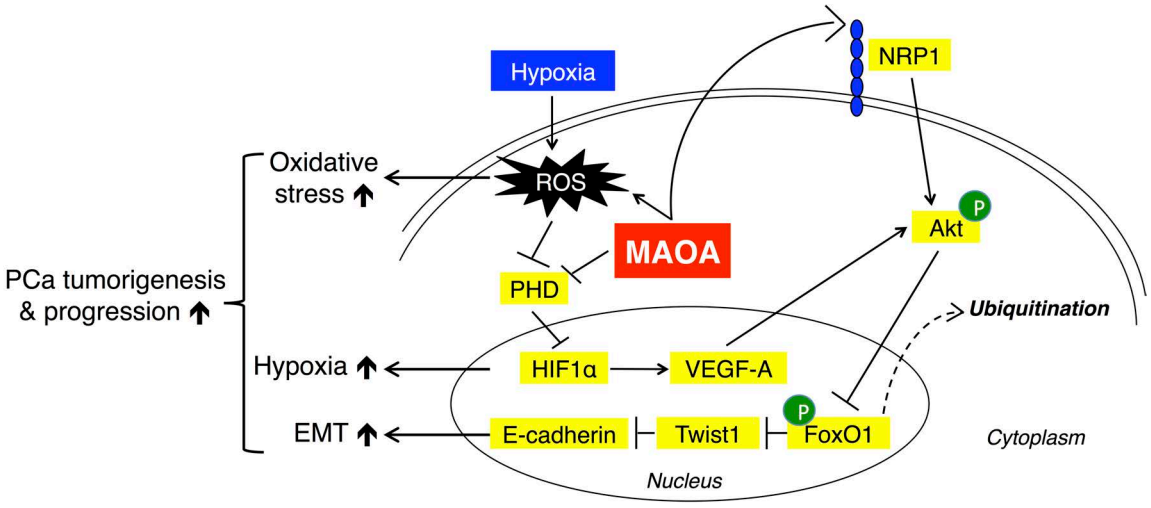
Hypoxia
NRP1
Oxidative stress
ROS
MAOA
Akt
P
PHD
Ubiquitination
PCa tumorigenesis & progression
Hypoxia
HIF1α
VEGF-A
EMT
E-cadherin
Twist1
P
FoxO1
Cytoplasm
Nucleus

Wu et al Fig 9